

NEUROPROTECTIVE EFFECT OF INTRANASAL DELIVERY OF ASIATIC ACID AGAINST
AMYLOID BETA₁₋₄₂-INDUCED ALZHEIMER'S DISEASE IN MICE



A Dissertation Submitted in Partial Fulfillment of the Requirements
for the Degree of Doctor of Philosophy in Pharmacology and Toxicology

Department of Pharmacology and Physiology

FACULTY OF PHARMACEUTICAL SCIENCES

Chulalongkorn University

Academic Year 2022

Copyright of Chulalongkorn University

ผลปกป้องประสาทของกรดเอเซียติกที่ให้ทางจมูกต่อโรคอัลไซเมอร์
ที่เหนียวนำด้วยอะมัยลอยด์เบต้า₁₋₄₂-ในหนูเมาส์



วิทยานิพนธ์นี้เป็นส่วนหนึ่งของการศึกษาตามหลักสูตรปริญญาเภสัชศาสตรดุษฎีบัณฑิต
สาขาวิชาเภสัชวิทยาและพิษวิทยา ภาควิชาเภสัชวิทยาและสรีรวิทยา
คณะเภสัชศาสตร์ จุฬาลงกรณ์มหาวิทยาลัย
ปีการศึกษา 2565
ลิขสิทธิ์ของจุฬาลงกรณ์มหาวิทยาลัย

Thesis Title NEUROPROTECTIVE EFFECT OF INTRANASAL DELIVERY
OF ASIATIC ACID AGAINST AMYLOID BETA₁₋₄₂-INDUCED
ALZHEIMER'S DISEASE IN MICE

By Mr. Ridho Islamie

Field of Study Pharmacology and Toxicology

Thesis Advisor Associate Professor RATCHANEE RODSIRI, Ph.D.

Accepted by the FACULTY OF PHARMACEUTICAL SCIENCES, Chulalongkorn
University in Partial Fulfillment of the Requirement for the Doctor of Philosophy

..... Dean of the FACULTY OF
PHARMACEUTICAL SCIENCES
(Professor PORNANONG ARAMWIT, Ph.D.)

DISSERTATION COMMITTEE

..... Chairman
(Associate Professor Jariya Umka Welbat, Ph.D.)

..... Thesis Advisor
(Associate Professor RATCHANEE RODSIRI, Ph.D.)

..... Examiner
(Associate Professor Thongchai Sooksawate, Ph.D.)

..... Examiner
(Assistant Professor VUDHIPORN LIMPRASUTR, D.V.M.,
Ph.D.)

..... Examiner
(NONTANETH NALINRATANA, Ph.D.)

รศ. อิสลามิ : ผลปกป้องประสาทของกรดอะซีติกที่ให้ทางจมูกต่อโรคอัลไซเมอร์ที่เหนี่ยวนำด้วยอะมัยลอยด์เบต้า₁₋₄₂ ในหนูเมาส์. (NEUROPROTECTIVE EFFECT OF INTRANASAL DELIVERY OF ASIATIC ACID AGAINST AMYLOID BETA₁₋₄₂-INDUCED ALZHEIMER'S DISEASE IN MICE) อ.ที่ปรึกษาหลัก : รศ. ภญ.ดร.รัชณี รอดศิริ

กรดอะซีติกเป็นสารออกฤทธิ์จากบัวบก (*Centella asiatica*) กรดอะซีติกมีฤทธิ์ปกป้องประสาทในโรคความผิดปกติของระบบประสาทส่วนกลางหลายโรค การเข้าสมองของกรดอะซีติกมีข้อจำกัดเนื่องจากกรดอะซีติกมีค่าชีวปริมาณออกฤทธิ์ต่ำ การพัฒนาระบบนำส่งทางจมูกของกรดอะซีติกใน solid lipid nanoparticle (SLN) ทำเพื่อเพิ่มการเข้าสู่สมองของกรดอะซีติก การวิจัยนี้มีวัตถุประสงค์เพื่อศึกษาผลปกป้องประสาทและกลไกการปกป้องประสาทของกรดอะซีติกใน SLN ที่นำส่งจากจมูกสู่สมองในหนูเมาส์ที่ถูกเหนี่ยวนำให้มีความจำบกพร่องด้วยอะมัยลอยด์เบต้า₁₋₄₂ ($A\beta_{1-42}$) แป้งหนูเมาส์พันธุ์ ICR เป็น 6 กลุ่มได้แก่ Sham, AD, AD-DON, AD-INAA, AD-POAA3 and AD-POAA30 ฉีด aggregated $A\beta_{1-42}$ เข้าโพรงสมองบริเวณ lateral แก่หนู AD ส่วนหนูกลุ่ม Sham ฉีด 10% dimethylsulfoxide (DMSO) in normal saline solution (NSS) 1 วันหลังจากฉีด $A\beta_{1-42}$ หนูกลุ่ม Sham และ AD ได้รับ 0.5% carboxymethylcellulose (CMC) (1 มก./กน., p.o.) ส่วนหนูกลุ่ม AD-DON, AD-INAA, AD-POAA3 และ AD-POAA30 ได้รับ donepezil (3 มก./กน., p.o.), AA in SLNs (2.04 ± 0.16 มก./กน., i.n.), AA (3 และ 30 มก./กน., p.o) ตามลำดับ ให้สารทดสอบติดต่อกัน 28 วัน ยกเว้น donepezil ให้เฉพาะวันที่ทำการทดสอบพฤติกรรมความจำ ทำการทดสอบ open field-test วันที่ 7 และ 18 novel object recognition (NOR) วันที่ 19-20 elevated-plus maze วันที่ 21 และ Morris water maze (MWM) วันที่ 22-27 เก็บสมอง 24 ชั่วโมงหลังจากการให้สารทดสอบครั้งสุดท้ายสำหรับวัดการแสดงออกของโปรตีน phosphorylated tau (pTau), การกระตุ้นของเซลล์เกลียซึ่งวัดโดยการย้อม gliol fibrillary acidic protein (GFAP) และ transmembrane protein 119 (TMEM119) ของเซลล์ประสาท, ระดับ IL-1b, TNF-a และ malondialdehyde (MDA) level, การสะสมของ $A\beta$ และจำนวนเซลล์ประสาท ผลการทดลองพบว่าการเรียนรู้และความจำแบบ spatial และแบบ recognition ของหนูกลุ่ม AD ลดลงอย่างมีนัยสำคัญทางสถิติ ส่วนหนูที่ได้รับกรดอะซีติกทางจมูกในหนูกลุ่ม AD-INAA สามารถบรรเทาความจำบกพร่องได้อย่างมีนัยสำคัญทางสถิติเมื่อเปรียบเทียบกับหนูกลุ่ม AD ในวันที่ 2-5 ของการทดลอง MWM (escape latency: $p < 0.01$, $p < 0.05$, $p < 0.001$ และ $p < 0.01$ ตามลำดับ; swimming distance: $p < 0.001$, $p < 0.01$, $p < 0.001$ และ $p < 0.001$ ตามลำดับ) และในช่วงการทดสอบของการทดลอง NOR (discrimination and preference index: $p < 0.05$ และ $p < 0.05$ ตามลำดับ) หนูกลุ่ม AD-POAA30 ก็มี escape latency และ swimming distance ในวันที่ 4 และ 5 ของการทดลอง MWM ลดลงอย่างมีนัยสำคัญทางสถิติ (escape latency: $p < 0.01$ และ $p < 0.01$ ตามลำดับ; swimming distance: $p < 0.001$ และ $p < 0.001$ ตามลำดับ) และมี discrimination index และ preference index ในการทดลอง NOR เพิ่มขึ้นอย่างมีนัยสำคัญทางสถิติเมื่อเปรียบเทียบกับหนูกลุ่ม AD ($p < 0.05$ และ $p < 0.05$ ตามลำดับ) ในขณะที่หนูกลุ่ม AD-POAA30 ภาวะความจำบกพร่องในการทดลอง MWM และ NOR ไม่ดีขึ้น การได้รับกรดอะซีติกทางจมูกและกรดอะซีติกทางปากขนาด 30 มก./กน. ลดการแสดงออกของโปรตีน pTau Serine-396 ($p < 0.05$ และ $p < 0.05$ ตามลำดับ) และ pTau Threonine-231 ($p < 0.01$ และ $p < 0.001$ ตามลำดับ) อย่างมีนัยสำคัญทางสถิติในสมองส่วนฮิปโปแคมปัส ลดการแสดงออกของโปรตีน GFAP และ TMEM119 ในบริเวณ CA1 (INAA: $p < 0.001$ และ $p < 0.05$ ตามลำดับ; POAA30: $p < 0.001$ สำหรับ GFAP) และบริเวณ CA3 (INAA: $p < 0.01$ และ $p < 0.05$ ตามลำดับ; POAA30: $p < 0.01$ สำหรับ GFAP) ของฮิปโปแคมปัส, ลดระดับ IL-1b ($p < 0.001$ และ $p < 0.001$ ตามลำดับ), TNF-a ($p < 0.05$ สำหรับ POAA30) และ ระดับ MDA levels ($p < 0.05$ และ $p < 0.05$ ตามลำดับ) ในเนื้อเยื่อสมอง อย่างไรก็ตามการฉีด $A\beta_{1-42}$ ไม่เหนี่ยวนำให้เกิดการตายของเซลล์ประสาทในฮิปโปแคมปัส โดยสรุปการให้กรดอะซีติกทางจมูกมีผลปกป้องประสาทจากพิษของ $A\beta_{1-42}$ ในสัตว์ทดลอง กลไกการปกป้องประสาทเกี่ยวข้องกับการยับยั้ง hyperphosphorylated tau protein ป้องกันการกระตุ้นเซลล์เกลียและการหลั่ง proinflammatory cytokine และลดการเกิด lipid peroxidation การวิจัยนี้แสดงให้เห็นว่าการให้กรดอะซีติกในรูปแบบ SLN ทางจมูกมีศักยภาพในการพัฒนาไปเป็นยาที่ใช้ในการรักษาโรคอัลไซเมอร์

CHULALONGKORN UNIVERSITY

สาขาวิชา เกษษัตริยาและพืชวิทยา
ปีการศึกษา 2565

ลายมือชื่อนิสิต
ลายมือชื่อ อ.ที่ปรึกษาหลัก

6273010933 : MAJOR PHARMACOLOGY AND TOXICOLOGY

KEYWORD: Asiatic acid, amyloid beta, alzheimer's disease, intranasal

Ridho Islamie : NEUROPROTECTIVE EFFECT OF INTRANASAL DELIVERY OF ASIATIC ACID AGAINST AMYLOID BETA₁₋₄₂-INDUCED ALZHEIMER'S DISEASE IN MICE. Advisor: Assoc. Prof. RATCHANEE RODSIRI, Ph.D.

Asiatic acid (AA) is an active natural compound that can be derived from *Centella asiatica* extract. Several pharmacological studies were reported that AA has potential as neuroprotector in the central nervous system disorders. AA penetration in the brain was limited due to its low bioavailability. Nasal delivery system of solid lipid nanoparticles (SLNs) loaded-AA was developed to increase AA penetration in the brain. The current study aimed to investigate neuroprotective effect and protective mechanisms of AA in SLNs by nasal-to-brain delivery technique against A β ₁₋₄₂ induced memory impairment by *in vivo* study. Male ICR mice were divided into six groups (n=11-12/group); Sham, AD, AD-DON, AD-INAA, AD-POAA3 and AD-POAA30. Aggregated A β ₁₋₄₂ was injected into lateral ventricle of all AD mice while Sham mice was injected with 10% Dimethylsulfoxide (DMSO) in normal saline solution (NSS). One day after A β ₁₋₄₂ injection, Sham and AD mice received 0.5% carboxymethylcellulose (CMC) (1 mL/kg, p.o.) while donepezil (3 mg/kg, p.o.), AA in SLNs (2.26 mg/kg, i.n.), AA (3 and 30 mg/kg p.o) were given to AD-DON, AD-INAA, AD-POAA3 and AD-POAA30, respectively. The treatments were given 28 consecutive days, 60 min before the behaviour test except donepezil was given only during memory behaviour test (7 days). Open field-test (OFT) was performed on days 7 and 18 followed by novel object recognition (NOR) on days 19-20, elevated-plus maze (EPM) on day 21, and Morris water maze (MWM) on days 22-27. 24-hours after the last treatment, brains were collected for further analysis of phosphorylated tau (pTau) protein expression, glial activation (detected by glial fibrillary acidic protein (GFAP) and transmembrane protein 119 (TMEM119)), proinflammatory cytokines (IL-1b and TNF-a) level, malondialdehyde (MDA) level, amyloid beta deposits and neuronal counts. The results showed that spatial learning memory and recognition memory of AD mice significantly reduced, while INAA treatment significantly alleviated memory deficits in AD-INAA mice compared AD mice on days 2-5 of MWM (escape latency: p < 0.01, p < 0.05, p < 0.001 and p < 0.01, respectively; swimming distance: p < 0.001, p < 0.01, p < 0.001 and p < 0.001, respectively) and on the testing phase of NOR (discrimination and preference index: p < 0.5 and p < 0.5, respectively). INAA treatment also significantly reduced pTau Serine-396 (p < 0.5) and pTau Threonine-231 (p < 0.01) protein expression in the hippocampus, GFAP and TMEM119 immunoreactivity in CA1 (p < 0.001 and p < 0.5, respectively) and CA3 (p < 0.01 and p < 0.5, respectively) subregion of the hippocampus, IL-1b (p < 0.001) and MDA levels (0.5) in the brain tissue. Additionally, A β ₁₋₄₂ injection did not induce neuronal loss in the hippocampus. To summarize, INAA had neuroprotective effect against A β ₁₋₄₂ *in vivo*. The underlying neuroprotective mechanisms are hyperphosphorylated tau protein inhibition, prevention of glial activation and proinflammatory cytokines and lipid peroxidation reduction. Taken together, the present study suggest that nasal delivery of AA in SLNs is a potential in drug development for the treatment of Alzheimer's disease

จุฬาลงกรณ์มหาวิทยาลัย
CHULALONGKORN UNIVERSITY

Field of Study: Pharmacology and Toxicology

Student's Signature

Academic Year: 2022

Advisor's Signature

ACKNOWLEDGEMENTS

First and foremost, I would like to deeply thank my research supervisor Associate Professor Ratchanee Rodsiri, Ph.D. for giving me the opportunity to do research and providing high quality of guidance and knowledge. It was a great privilege and honour to study under her supervision. Her patience, empathy, and encouragement are the most valuable support to help accomplish my degree. I also would like to express my sincere gratitude to Professor Garnpimol Ritthidej, Department of Pharmaceutics and Industrial Pharmacy, Faculty of Pharmaceutical Sciences, Chulalongkorn University for kindly supporting Asiatic acid loaded SLNs solution for my project. I also would like to thank my thesis committee Assoc. Prof. Jariya Umka Welbat, Ph.D., Assoc. Prof. Thongchai Sooksawater, Assist. Prof. Vudhiporn Limprasutr, D.V.M., Ph.D., and Nonthaneth Nalinratana, Ph.D. for their comments, encouragement, and insightful questions and suggestions. I also would also like to thank my special family member, especially my lovely wife Mrs. Ratna Efa Agustin, for always believing and take care our children, my daughter Kirana and my son Kirandra who always made my day better than yesterday. Special thanks to my dad and mom for their love, supporting, understanding, and caring. I also would like to thank my labmates: Miss. Su Lwin, Miss. Saranda, Miss. Hattaya for helping me about the lab work. Also, I thank my friends Mr. Iksen, Mr. Aditya Mr. Hasriadi, and Mrs. Andita for their support and encouragement during my Ph.D study. I am also grateful to the Second century (C2F) scholarships for giving me the funding source that allowed me to pursue my graduate school study. Last but not least, I would like to express my gratitude to everyone who has assisted and supported me in completing my degree directly or indirectly.

จุฬาลงกรณ์มหาวิทยาลัย
CHULALONGKORN UNIVERSITY

Ridho Islamie

TABLE OF CONTENTS

	Page
ABSTRACT (THAI)	iii
ABSTRACT (ENGLISH)	iv
ACKNOWLEDGEMENTS	v
TABLE OF CONTENTS	vi
List of Tables	x
List of Figures.....	xi
ABBREVIATIONS.....	i
CHAPTER 1.....	1
INTRODUCTION.....	1
1.1 Background and Rationale.....	1
1.2 Research Questions.....	3
1.3 Objectives	3
1.4 Hypothesis	3
1.5 Research design.....	4
1.6 Benefits of Study	4
1.7 Conceptual Framework.....	4
CHAPTER 2.....	5
LITERATURE REVIEW	5
2.1 Memory	5
2.2 Alzheimer’s Disease.....	7
2.3 Pathophysiology of Alzheimer’s Disease.....	8

2.3.1 Amyloid-Beta Plaque	8
2.3.2 Tau Hyperphosphorylation	9
2.3.3 Neuroinflammation.....	10
2.3.4 Oxidative Stress	13
2.4 Asiatic Acid.....	13
2.5 Intranasal Delivery System	16
2.6 Solid Lipid Nanoparticles (SLNs).....	19
CHAPTER 3.....	22
MATERIALS AND METHODS	22
3.1 Materials.....	22
3.1.1 Chemicals and Reagents	22
3.1.2 Equipments	24
3.1.3 Drug Preparation	25
3.1.4 Preparation of Amyloid-Beta ₁₋₄₂ oligomers	25
3.1.5 Animals.....	27
3.2 Methods	27
3.2.1 Experimental design	27
3.2.2 Intracerebroventricular Injection of Amyloid Beta ₁₋₄₂	30
3.2.3 Behavioural Tests.....	31
3.2.3.1 Open-Field Test (OFT)	31
3.2.3.2 Novel Object Recognition Test (NORT)	32
3.2.3.3 Elevated Plus Maze (EPM)	33
3.2.3.4 Morris Water Maze (MWM).....	34
3.2.4 Brain Collection.....	35

3.2.5 Western Blot Analysis	36
3.2.6 Enzyme-linked Immunosorbent Assay (ELISA).....	37
3.2.7 Lipid Peroxidation Assay.....	38
3.2.8 Histology Analysis	39
3.2.8.1 Immunohistochemistry.....	39
3.2.8.2 Immunofluorescence.....	40
3.2.8.3 Nissl Staining.....	42
3.3 Data Analysis.....	43
CHAPTER 4.....	44
RESULTS.....	44
4.1 The protective effect of nasal delivery and oral administration of AA against spatial memory dysfunction induced by $A\beta_{1-42}$	44
4.2 The protective effect of nasal delivery and oral administration of AA against recognition memory dysfunction induced by $A\beta_{1-42}$	48
4.3 The effect of $A\beta_{1-42}$ and AA on exploratory behaviour in mice	51
4.4 The effect of $A\beta_{1-42}$ and AA on the anxiety-like behaviour in mice.....	53
4.5 The protective effect of nasal delivery and oral administration of AA against tau hyperphosphorylation induced by $A\beta_{1-42}$	55
4.6 The protective effect of nasal delivery and oral administration of AA against glial activation induced by $A\beta_{1-42}$	58
4.7 The protective effect of nasal delivery and oral administration of AA against the increased proinflammatory cytokines level induced by $A\beta_{1-42}$	62
4.8 The protective effect of nasal delivery and oral administration of AA against lipid peroxidation induced by $A\beta_{1-42}$	63
4.9 The effect of $A\beta_{1-42}$ and AA treatment on the neuronal cell counts.....	64

CHAPTER 5.....	66
DISCUSSION AND CONCLUSION	66
REFERENCES	74
APPENDIX 1	98
Animal Use Certificate	98
VITA.....	99



List of Tables

	Page
Table 1 Advantages and limitation of the intranasal delivery system.....	19
Table 2 Animal group and the treatment	30
Table 3 Nissl staining step-by-step protocol.	42



List of Figures

	Page
Figure 1 Molecular structure of Asiatic Acid.....	15
Figure 2 $A\beta_{1-42}$ fragments before and after 96-hr incubation at 37°C.	26
Figure 3 Experimental timeline of the neuroprotective effect of AA	29
Figure 4 The direct intracerebroventricular (i.c.v.) injection of $A\beta_{1-42}$	31
Figure 5 Experimental design for novel object recognition test.....	33
Figure 6 Diagram of a circular pool in Morris water maze	35
Figure 7 Distribution profile of $A\beta_{1-42}$ in the hippocampus of mice.....	40
Figure 8 The effect of AA by intranasal and oral administration on the spatial memory dysfunction induced by $A\beta_{1-42}$ in the Morris water maze test.....	46
Figure 9 The effect of AA by intranasal and oral administration on the long-term memory dysfunction induced by $A\beta_{1-42}$ in the Morris water maze test.....	47
Figure 10 The effect of AA by intranasal and oral administration on the recognition memory impairment induced by $A\beta_{1-42}$ in the novel object recognition test.....	50
Figure 11 The effect of $A\beta_{1-42}$ and AA treatment on exploration activity in the open-field test	52
Figure 12 The effect of $A\beta_{1-42}$ and AA treatment on the anxiety-like behavior	54
Figure 13 The effect of AA by intranasal and oral administration on tau hyperphosphorylation induced by $A\beta_{1-42}$	57
Figure 14 The effect of AA by intranasal and oral administration on glial activation induced by $A\beta_{1-42}$ in the CA1 of hippocampus.	60
Figure 15 The effect of AA by intranasal and oral administration on glial activation induced by $A\beta_{1-42}$ in the CA3 of hippocampus.	61

Figure 16 The effect of AA by intranasal and oral administration on the increased IL- 1β (A) and TNF- α (B) levels induced by A β_{1-42}	63
Figure 17 The effect of AA by intranasal and oral administration on MDA levels in the mice brain induced by A β_{1-42}	64
Figure 18 The effect A β_{1-42} injection and AA treatment on the neuronal counts in the hippocampus.....	65



ABBREVIATIONS

α = Alpha

β = Beta

pTau = phosphorylated tau

$^{\circ}\text{C}$ = Degree Celsius

μL = microliter(s)

/ = per

% = percentage

\pm = plus-minus sign

AD = Alzheimer's Disease

ANOVA = analysis of variance

BSA = bovine serum albumin

BBB = blood brain barrier

B.W = body weight

CAT = catalase

CMC = carboxy methyl cellulose

CNS = central nervous system

CYP450 = cytochrome P450

g = gram(s)

GAPDH = glyceraldehyde 3-phosphate dehydrogenase h=hour



GFAP = glial fibrillary acidic protein

HCl = hydrochloric acid

IC₅₀ = half maximum inhibitory concentration

i.p = intraperitoneal injection

i.n = intranasal administration

kg = kilogram(s)

MDA = malondialdehyde

mg = milligram(s)

mL = milliliter(s)

n = number

NSS = normal saline solution

PBS = phosphate buffer saline

pH = potential of hydrogen ion

p.o = per os, oral administration

ROS = reactive oxygen species

SDS = sodium dodecyl sulfate

SLN = solid lipid nanoparticle

S.E.M = standard error of mean

SOD = superoxide dismutase

TBA = thiobarbituric acid

TBARS = thiobarbituric acid reacting substances



จุฬาลงกรณ์มหาวิทยาลัย
CHULALONGKORN UNIVERSITY

TMEM119 =transmembrane protein 119



CHAPTER 1

INTRODUCTION

1.1 Background and Rationale

Alzheimer's disease (AD) is the most prominent form of dementia in elderly patients. The main pathological hallmarks of AD includes amyloid-beta ($A\beta$) plaque and neurofibrillary tangles (NFTs)¹ followed by neuronal loss² that leads to the formation of cortical atrophy in the brain. Several pathogenesis are involved in $A\beta$ -induced neurotoxicity including neuroinflammation³ and oxidative stress⁴. Current standard therapy of AD such as cholinesterase inhibitors and NMDA receptor antagonists is limited to symptomatic treatment⁵. The causes of neuronal damage in AD are not the main target of these drugs. Therefore, alternative strategies are needed in order to develop a modified therapy that targeting neuropathological mechanisms of AD.

Asiatic acid (AA) is a natural bioactive compound extracted from *Centella asiatica* L. AA is a potential neuroprotective agent. Pharmacological effects of AA in the central nervous system (CNS) disorders have been investigated *in vitro* and *in vivo*. The protective effects of AA have been elucidated against $AlCl_3$ ⁶, glutamate^{7,8} and methamphetamine⁹ induced cytotoxicity in the neuronal cell lines. Additionally, AA improved learning and memory dysfunction induced by $AlCl_3$ ¹⁰,

quinolinic acid¹¹, 5-fluorouracil¹² and valproate¹³ in rodents. However, the oral bioavailability of AA in rats was as low as 16.25% due to rapid metabolism by cytochrome P450 (CYP)¹⁴. In order to increase the availability of AA in the brain, the alternative strategies are required to improve its pharmacological effect.

Nasal delivery technique has been developed to enhance AA penetration into the brain. Intranasal delivery system is a rapid, safe, and non-invasive technique that produce quick onset of action due to rapid drug absorption¹⁵. Several drug compounds that act on CNS including olanzapine¹⁶, venlafaxine¹⁷, carbamazepine¹⁸, and donepezil¹⁹ have been developed for nose-to-brain delivery system. In addition, the intranasal administration of diazepam²⁰, midazolam²¹, insulin²², angiotensin II²³, melanocortin proteins²⁴, oxytocin²⁵, and orexin-A²⁶ have shown their efficacy in the clinical trials.

In this study, solid lipid nanoparticles (SLNs) formulation was applied to enhance AA absorption in the nasal cavity. This formulation is promising strategy to improve nasal absorption of drug molecule and increase the effectiveness of nose-to-brain delivery system leading to an increase of drug's availability in the brain²⁷. Several studies have demonstrated the efficacy of nasal delivery of SLNs formulation for various CNS drug including donepezil²⁸ haloperidol²⁹ risperidone³⁰. In addition, the previous study has been developed various formulations of SLNs-loaded AA and tested in the nasal cell line³¹. Previous study showed that intranasal delivery of AA in SLNs improve learning and memory impairment induced by scopolamine³². This

study aimed to evaluate the neuroprotective effect of intranasal delivery of AA in SLNs and its underlying protective mechanisms against $A\beta_{1-42}$ induced AD mice model.

1.2 Research Questions

1. Does intranasal of AA improve learning and memory impairment induced by $A\beta_{1-42}$?
2. What are the neuroprotective mechanisms of AA?

1.3 Objectives

1. To investigate the neuroprotective effects of AA given by intranasal delivery in the AD mouse model induced by $A\beta_{1-42}$.
2. To investigate the neuroprotective mechanisms of AA against $A\beta_{1-42}$ induced neurotoxicity including the inhibition of hyperphosphorylated Tau protein, oxidative stress and neuroinflammation in the AD mouse model.

1.4 Hypothesis

Intranasal delivery of AA improves learning and memory and protect neuronal loss through the inhibition of hyperphosphorylated Tau protein, oxidative stress and neuroinflammation in AD mice model induced by $A\beta_{1-42}$.

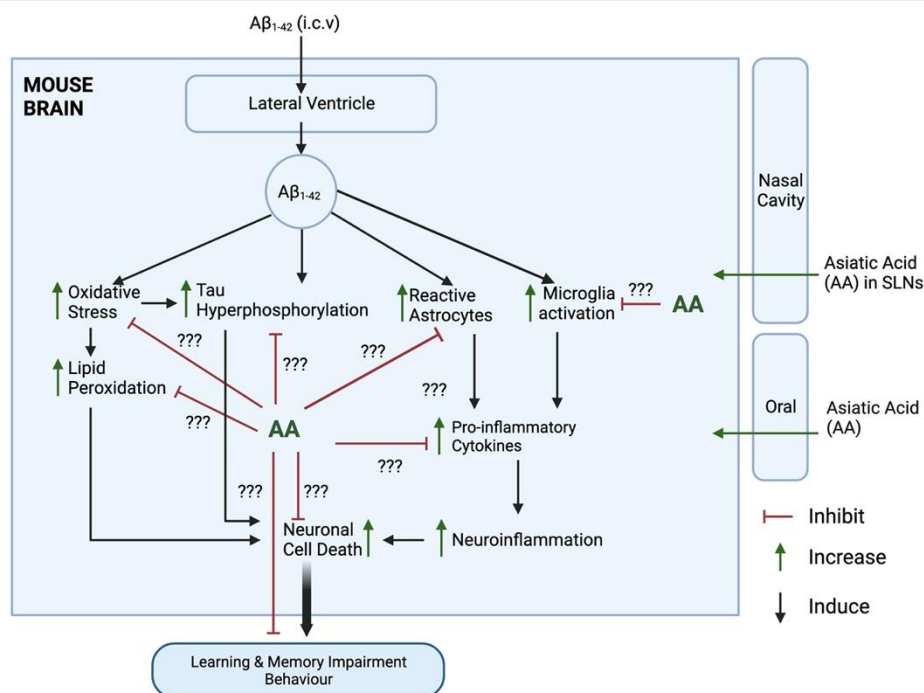
1.5 Research design

Experimental design

1.6 Benefits of Study

The expected benefit of this study is to provide scientific information on the neuroprotective effect of intranasal delivery of AA and the neuroprotective mechanisms of AA against memory impairments induced by intracerebroventricular $A\beta_{1-42}$ injection. This information will be supported the further development of the AA nasal delivery system for the treatment of Alzheimer's disease.

1.7 Conceptual Framework



CHAPTER 2

LITERATURE REVIEW

2.1 Memory

Memory is the retention of previously acquired knowledge or new information. According to time, memory is divided into short-term and long-term memory³³. Moreover, memory can be also classified into several kinds including working memory, spatial memory, and procedural memory. Short-term and working memory can be converted into long-term memory by the consolidation process^{33,34}.

Different brain areas are mediated in each type of memory in humans and rodents. Working memory has a small capacity in the brain. Some sensory information such as the serial phone number that we need to recall is regulated by this type of memory³⁵. The prefrontal cortex is the main area responsible to control the working memory³⁵. The medial prefrontal cortex (mPFC) is the main subregion in the PFC that has an essential role in the storage of working memory³⁶. Long-term memory is the memory that can be recalled for days, months or years after its storage in the memory system. The ability to remember the direction is one of sensory information that regulate by this memory system called “long-term spatial memory”³⁵. Long-term memory is mainly regulated by the hippocampus (HPC) located in the medial temporal lobe³⁷. Long-term potentiation in the *cornu ammonis*

1 (CA1) area in the hippocampus is the major area that responsible for consolidation process of short-term and working memory³⁵. In addition, ventral hippocampus (vHPC) has a direct connection with the mPFC through entorhinal cortex^{38,39}. By this connection, HPC and PFC are hypothesized to be involved in the consolidation process of working memory.

Memory behavior in rodents can be evaluated using various methods including Morris water maze, Barnes maze, T-maze, Y-maze, and Radial Arm maze⁴⁰. These methods are commonly employed in laboratory settings to assess spatial learning and memory in rodents, particularly mice⁴⁰. The Morris water maze is a well-known test used to evaluate spatial learning and memory in rodents. In this test, animals are placed in a large pool of water and must learn to locate a hidden platform using visual-spatial cues. The time taken to find the platform and the path taken are measured as indicators of spatial memory performance^{41,42}. In addition to spatial memory, working and recognition memory, can be evaluated using Novel object recognition test (NOR)⁴³. The novel object recognition test is a widely used behavioural assay for studying memory formation and cognitive processes in rodents⁴³. This test involves assessing an animal's ability to recognize and remember a previously encountered object when presented with a novel object^{43,44}. The principle of NOR test is based on the natural tendency of rats and mice to explore the novel objects more than the familiar ones^{43,44}

2.2 Alzheimer's Disease

Alzheimer's disease is the most common cause of dementia that contribute around 60-70% of cases. World Health Organization (WHO) estimated about 55 millions people to live with dementia in 2021 and predicted that it will be reached 78 millions people by 2030 and 139 millions by 2050⁴⁵. Based on the onset of the disease, AD is divided into 2 types: early-onset (also known as familial AD) and late-onset (also known as sporadic AD). The prevalence of familial AD is relatively rare (less than 5% of total AD cases) compared to sporadic AD (more than 95% of total AD cases)⁴⁶. The risk factors of AD are age, gender, genetics, traumatic brain injury, diet, obesity, etc⁴⁷. Clinically, losses of short-term memory and working memory are the first symptoms commonly detected at the early-stage AD patients. Furthermore, learning impairments followed by long-term memory deficits are affected at the later stage of AD^{46,47}.

The current pharmacological treatment of AD is limited. Two drug classes, cholinesterase inhibitors (e.g., donepezil) and NMDA receptor antagonists, (e.g., memantine) are used for symptomatic therapy in AD⁵. They do not target the main pathology of AD. New approaches in the treatment of AD are needed to overcome this problem. In June 2021, United State Food and Drug Administration (U.S. FDA) has approved aducanumab (marketed as Adulhem) as the disease-modifying drug for the treatment of AD. Aducanumab is a monoclonal antibody which can reduce amyloid-

beta plaques in the brain by increasing amyloid beta clearance. As an antibody, Aducanumab can react to amyloid beta aggregates, insoluble fibrils and soluble amyloid beta oligomers selectively by binding to the specific amino acid residue in the amyloid beta structure⁴⁸. Neuroprotection is another therapeutic approach for disease-modifying by delayed neuronal death, and consequently delayed disease progression. In this study, the potential neuroprotective compound, asiatic acid, was investigated its effects at the targets of the main neuropathological hallmarks in AD and the molecular mechanisms underlying the pathological processes of AD.

2.3 Pathophysiology of Alzheimer's Disease

2.3.1 Amyloid-Beta Plaque

The main pathological hallmark of AD is extracellular amyloid- β ($A\beta$) plaque. $A\beta$ is the degradation product of amyloid precursor protein (APP)^{1,49}. An increase in production or a decrease in the clearance of $A\beta$ leads to the accumulation of the plaques^{1,50}. APP is cleaved by two main pathways; the amyloidogenic and non-amyloidogenic pathways. In the non-amyloidogenic pathway, APP is cleaved by α and γ -secretases, which produces soluble fragment $sAPP\alpha$ and C-terminal (C-99) fragment. In the amyloidogenic pathway, APP is cleaved by β and γ -secretases, which produces soluble fragment $sAPP\beta$, C-terminal fragment, and $A\beta$ ⁵¹.

Two major isoforms of A β fragments are commonly found in AD patients: A β ₁₋₄₀ and A β ₁₋₄₂⁵². A β ₁₋₄₂ has two extra residues at the C-terminus which make A β ₁₋₄₂ aggregate faster and more neurotoxic than A β ₁₋₄₀. A β ₁₋₄₂ is also the major isoform of amyloid plaques in AD brains⁵³. The A β fragment is a sticky-forming plaque that blocks the signalling pathway between synapses, resulting in synaptic dysfunction. A β plaque formation occurs mainly in the hippocampus, the brain area that regulates memory function, and also in the cerebral cortex, which controls the cognitive function and decision-making. Furthermore, A β plaque causes tau protein hyperphosphorylation, loss of synapses, neuronal apoptosis, brain vascular damage, and neuroglial activation⁵⁴.

2.3.2 Tau Hyperphosphorylation

Tau, a microtubule-associated protein, is the main regulator of microtubule assembly in the neurons. Tau structure is divided into 2 main domains including the projection domain and microtubule-binding domain⁵⁵. Tau mediates microtubule stabilization, regulation of axonal diameter and transport, and neurogenesis⁵⁶. Together with microfilaments and intermediate filaments, the microtubule builds the cytoskeleton in the neurons. Microtubule stability is controlled by post-translational modification of tau protein such as phosphorylation, O-glycosylation, ubiquitination, glycation, acetylation, etc^{56,57}. Phosphorylation is the major post-translational modification of neuronal tau protein. The affinity of tau protein to microtubule is

reduced by increasing tau phosphorylation and leads to destabilization of the cytoskeleton⁵⁸.

Hyperphosphorylation of tau protein is one of the main neuropathological hallmarks of AD. It can be induced by several mechanisms such as oxidative stress and neuroinflammation. Eighty-five phosphorylation sites of tau protein have been found in normal and AD brains^{59,60}. Serine and threonine residues in the microtubule-binding domain are the most common phosphorylation sites of the hyperphosphorylated tau protein of AD⁶¹. In the AD mice model, Ser-396 and Thr-231 are the most common sites of tau hyperphosphorylation induced by A β plaques⁶². Furthermore, Ser-396 and Thr-231 were also highly expressed in the CSF brain of AD patients^{59,63,64}.

The aggregation of hyperphosphorylated tau in neurons leads to the formation of intracellular neurofibrillary tangles (NFTs), impairs microtubule stability⁵⁸, disrupts axonal transportation and results in neuronal damage and synaptic loss⁶⁵. NFTs are most commonly found in the hippocampus and entorhinal cortex. They are found in other parts of the cerebral cortex in the advanced-stage AD⁶⁵.

2.3.3 Neuroinflammation

Neuroinflammation plays a significant role in the development of AD. Astrocytes and microglia are involved in the progression of neuroinflammation^{66,67}. In normal

brain, astrocytes and microglia are in the resting state. They become reactive in the presence of A β plaque in the early-stage AD⁶⁶.

Microglia are the phagocytic cells in the CNS. They protect the neurons by removing the cellular debris and pathogens⁶⁸. Other roles of microglia include maintaining neuronal circuits and supporting synapse remodelling⁶⁹. Microglia are activated by pathological triggers, such as protein aggregates, neuronal death, and then migrate to the site of injury to initiate the innate immune response. In AD, soluble A β oligomers and A β fibrils have an affinity to bind Toll-like receptors (TLR2, TLR4/CD14, TLR6 and TLR9) on the surface of microglia and trigger the innate immune response by producing proinflammatory cytokines (TNF- α , IL-1 β , IL-6, and IL-10) and chemokines. On the other hand, A β oligomers binding to other cell-surface receptors, such as SCARA1, α 6 β 1 integrins, CD36 and CD47, can initiate A β uptake into the microglia leading to A β clearance⁶⁶. In the later stage of AD, the phagocytic capacity of microglia is insufficient due to the downregulation of A β phagocytic receptors leading to the reduction of A β clearance^{50,70}.

Astrocytes are the highest glial cell populations in the CNS. It has several key functions in brain development such as maintaining the blood-brain barrier, homeostasis of ions, water, nutrients, trophic factors and synapse in neurons, and controlling the release and uptake of neurotransmitters⁷¹. Morphological change is the first sign of astrocyte activation. Following activated microglial, astrocyte atrophy

has been found in the presence of A β oligomers at the early stage of AD. Then, astrocytes become more reactive to surrounding A β plaques and change to a hypertrophic form which is mainly observed in the later stages of AD⁷². The atrophic and hypertrophic forms can be found in the post-mortem brain of AD patients⁷³ and in the AD animal models⁷⁴. In the AD mice model, astrocytes atrophy was found in the CA1 hippocampus in mice induced by intracerebroventricular injection of A β oligomers⁷⁵. In addition, reactive astrocytes significantly elevated levels of glial fibrillary acidic protein expression (GFAP)⁷⁶. Therefore, GFAP can be used as the marker of activated astrocytes in neuroinflammation. Like microglia, astrocytes also released pro-inflammatory mediators (cytokines, interleukins, nitric oxide and other neurotoxic components) after A β exposure^{67,72}.

Excessive production of proinflammatory cytokines induced neuronal death by several mechanisms. Proinflammatory cytokines also cause synaptic dysfunction and inhibit neurogenesis^{77,78}. IL-1 β causes synaptic loss by increasing prostaglandin E2 synthesis which leads to the release of presynaptic glutamate and excitotoxicity⁷⁸. In addition, TNF induces neuronal death by activating TNF receptor 1 (TNFR1) and inhibits the NF- κ B pathway by recruitment of caspase 8 to promote apoptosis^{79,80}. Furthermore, TNF- α and IL-1 β induced neuronal death by increased A β synthesis, increased tau hyperphosphorylation, and reduced long-term potentiation (LTP) which leads to the inhibition of synaptogenesis^{67,77,81}.

2.3.4 Oxidative Stress

Oxidative stress is an essential mechanism in the development of AD. Oxidative stress is an imbalance between reactive oxygen species (ROS) production and antioxidant system capacity⁸². ROS mainly generated by mitochondria during the electron transport chain (ETC) at the physiological level. Antioxidants and antioxidant enzymes such as superoxide dismutase (SOD), catalase (CAT), and glutathione, regulate the overproduction of ROS levels⁸².

Significant oxidative damage associated with the accumulation of A β and NFTs was presented in the brain of AD patients^{83,84}. Dysfunction of DNA, proteins and lipids are the impact of oxidative stress. A study has shown that A β ₁₋₄₂ is the most likely aggregated protein that produces hydrogen peroxide and other ROS⁸⁵. Membrane phospholipids in the brain is vulnerable to free radical attacks. Lipid peroxidation is one of the oxidative stress markers found predominantly in the AD brains⁸⁶. In another way, oxidative stress causes hyperphosphorylation of tau⁸⁷.

2.4 Asiatic Acid

Asiatic acid (AA) is a natural triterpenoid (Figure 1) extracted from *Centella asiatica* L. Various studies have demonstrated the pharmacological activities of AA *in vitro* and *in vivo*. AA has been shown its antioxidant and anti-inflammatory⁸⁸, anticancer⁸⁸, antimicrobial⁸⁹, antihyperlipidemic and antidiabetic⁹⁰, and

antihypertension⁹¹ effects. AA also has potential for the treatment of neuropathy⁹², Parkinson's disease⁹³ and Alzheimer's disease⁹⁴. AA improved learning and memory impairments induced by valproate¹³, 5-fluorouracil¹², quinolinic acid¹¹, and AlCl₃. The neuroprotective effects of AA have also been evaluated in Parkinson's disease⁹³, stroke^{95,96}, and ageing brain models⁹⁷. AA has a protective effect against cytotoxicity in the neuronal cell line exposed to neurotoxic compounds such as glutamate^{7,8}, methamphetamine⁹, and AlCl₃⁶.

Many studies have evaluated the molecular mechanisms of AA in Alzheimer's disease. *In vitro* and *in silico* studies showed that AA inhibited acetylcholinesterase (AChE) activity with IC₅₀ and binding energy values of 15.05 $\mu\text{g/mL}$ and -10.27 Kcal.mol⁻¹, respectively⁹⁸. AA decreased the expression of pro-inflammatory cytokines (IL-1 β , IL-6, IL-8, and TNF- α) and modulated immune responses through the activation of toll-like receptors⁹⁹. AA also attenuated AlCl₃-induced tau pathology, oxidative stress and apoptosis via AKT/GSK-3 β signalling pathway in rats¹⁰⁰. In addition, AA modulated several enzymatic pathways related to β -amyloid plaque formation, including down-regulated beta-secretase (BACE1) and up-regulated disintegrin and metalloproteinase domain-containing protein 10 (ADAM10), insulin-degrading enzyme (IDE) and neprilysin (NEP)¹⁰¹. Our previous study has shown that intranasal administration of AA at the dose of 2.31 ± 0.238 mg/kg can improve memory deficits induced by scopolamine³².

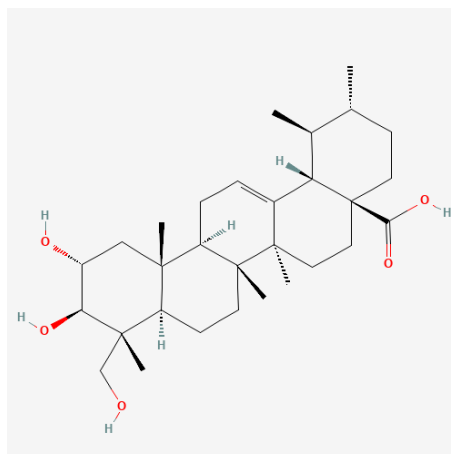


Figure 1 Molecular structure of Asiatic Acid

Pharmacokinetic (PK) profiles of AA have become a problem in the treatment of CNS diseases. The oral bioavailability of AA was 16.25%, with a half-life of 0.624 h in rats. This resulted from the rapid metabolism by hepatic enzymes CYP450¹⁴. AA is also a potent inhibitor of CYP2C9¹⁰². Hydroxylation and dehydrogenation are the main reaction of AA metabolism¹⁰³. Following oral administration in rats, AA showed the following PK parameters: T_{max} (0.5h), C_{max} (0.394ng mL⁻¹), $t_{1/2}$ (0.642h), $AUC_{(0-24)}$ (0.702ng mL⁻¹ h²), $AUC_{(0-\infty)}$ (0.766ng mL⁻¹ h²), $AUMC_{(0-24)}$ (1.213ng mL⁻¹ h²), $AUMC_{(0-\infty)}$ (1.641ng mL⁻¹ h²), CL (6.682 L h⁻¹), and MRT (0.668 h)¹⁴. AA molecule has poor aqueous solubility with 5.98x10⁻² mg/L at 25°C in water¹⁰¹. Therefore, to overcome this problem, solid lipid nanoparticle formulations of AA have been developed to enhance the brain penetration of AA. AA has a molecular weight of 488.709 g/mol which classify into a low molecular weight drug and it has high lipophilicity

($\log P = 5.7$)¹⁰¹. Thus, the high lipophilicity of AA will be beneficial in implementing the nose-to-brain delivery system.

2.5 Intranasal Delivery System

Intranasal administration is a promising method for delivering therapeutic compounds to CNS because it can reduce systemic exposure and also avoid undesirable reactions from drugs that act in the CNS¹⁰⁴. Intranasal administration of drugs in animal models is used to evaluate pharmacokinetic distribution as well as their pharmacodynamic profiles¹⁰⁵. Besides being able to minimize systemic exposure, this delivery route can increase patient compliance, ease of administration, and have a rapid onset of action¹⁵. Several CNS drugs have been developed for intranasal administration, including donepezil, venlafaxine, olanzapine and carbamazepine¹⁶⁻¹⁹. Additionally, certain medications such as diazepam, midazolam, insulin, angiotensin II, melanocortin proteins, oxytocin and orexin-A have been shown to be effective in clinical trials through the application of the nose-to-brain delivery system²⁰⁻²⁶.

A drug molecule reaches the brain via two main pathways after intranasal administration. First, a drug molecule enters the brain through the olfactory epithelium mediated by olfactory neurons. Second, a drug can be through the respiratory epithelium, where the drug must have the ability to penetrate BBB

and CSF to enter the brain after circulating in the bloodstream. These two epitheliums also have a connection with the trigeminal nerve that is in the posterior of the nasal cavity, which also has direct access to the brain¹⁰⁴. Drug molecules are transported from the nasal cavity to the brain's parenchyma along with the olfactory or trigeminal nerves. This process of transport can be achieved via intracellular and extracellular mechanisms. The endocytic vesicles traffic within the neuron to the projection site and the drug molecules inside the vesicles are released through exocytosis. On the other hand, the extracellular mechanism begins with the drug passing across the nasal epithelium towards the lamina propria leading to the axon in the CNS, where the drug is further dispersed through fluid movement¹⁰⁵. Trigeminal nerve pathway is divided into three divisions including the ophthalmic (V1), the maxillary (V2), and the mandibular division (V3). However, only neurons from V1 and V2 innervate to the nasal epithelium. Thus, both branches could play an essential role in nose to brain drug delivery¹⁰⁶. By using trigeminal nerve pathway, drug can be transported to the trigeminal nerve synapse at the pons level and subsequently distributed into other brain area. On the other hand, nose-to-brain drug delivery can occur by indirect mechanism in the respiratory epithelium, a rich-vascular region in the nasal cavity. Drug molecules can enter the bloodstream through the vascular epithelium and subsequently pass BBB to reach the brain parenchyma¹⁰⁶. As a

lipophilic molecule, AA has high ability to penetrate BBB and easily enter the brain by transcellular mechanism.

Several factors affecting the absorption of intranasal administration include physicochemical properties of drug molecules, formulation factors, factors related to delivery devices and biological factors¹⁵. Regarding to physicochemical factors, molecular weight and lipophilicity of drug molecules have a major role in the effectiveness of nose-to-brain delivery. Formulation factors needed to be considered are drug concentration, dose, and volume of administration¹⁵. Furthermore, mucociliary clearance and enzymatic degradation are biological factors that needed to be considered in implementing the nose-to-brain delivery system. Both factors are the main elimination mechanisms that can occur in drug molecules in the nasal mucosa¹⁰⁴. Other factors related to the biological aspect are the surface area of the olfactory region and the diameter of the axon.

The structure and morphology of the olfactory region are different between humans and mice. The olfactory region of humans covers approximately 1.25–10% of the nasal cavity's total surface area, which is 2–12.5 cm², with a mucus thickness of 60 μm^{107,108}. Meanwhile, the olfactory epithelium surface area of mice ranges between 1.25–1.40 cm² which covers about 50% of the nasal cavity¹⁰⁹. Moreover, the diameter of human olfactory axons is 0.1–0.7 μm¹¹⁰, while the olfactory nerve's axonal diameter in the lamina propria in three months old of ICR mice has been determined to range from 0.08–0.14 μm¹¹¹.

Table 1 Advantages and limitation of the intranasal delivery system

Advantages ¹¹²	Limitations ¹¹²
Non-invasive, safe, rapid delivery technique	Rapid elimination due to mucociliary clearance from nasal cavity
Avoid first-pass elimination and gut-wall metabolism	Mucosal toxicity can be appeared due to absorption enhancers used in the formulation
Bypass BBB results in reducing systemic exposure	There is a variability in the concentration attainable in different areas of the brain.
Rapid onset of action due to quick drug absorption	Decrease permeability of nasal mucosa due to high molecular weight of drugs.
Better patient adherence	Some drugs may induce nasal mucosa irritation
Served as alternative route for parenteral administration	Cold or allergic conditions may result nasal congestion then interfere the administration
Good bioavailability for low molecular weight drugs	Frequent use may induce mucosal damage leading to infection

2.6 Solid Lipid Nanoparticles (SLNs)

Solid lipid nanoparticles (SLNs) are lipid-based delivery systems. SLNs are typically found in a spherical shape with smooth surface and median sizes of 100-300 nm. Smaller (less than 100 nm) or larger (up to 1,000 nm) sizes may be presented in SLNs¹¹³. SLNs are prepared with lipids matrix or lipid combinations which remain in a solid-state at room and body temperature. Drug molecules are dissolved or dispersed inside the lipid matrix¹¹³. Preparation of SLNs can be

achieved by several methods, including high-pressure homogenization, hot homogenization, cold homogenization, emulsification technique and microemulsion technique¹¹⁴.

The advantages of SLNs include controlled and targeted drug release, increased stability of incorporated drugs, ease of production at a large scale, longer stability and decreased toxicity¹¹⁴. SLNs reduce the toxicity of the therapeutic molecules by protecting them from reticuloendothelial system clearance. The long-term stability of SLNs allows them to be used for long periods of time. SLNs can deliver both lipophilic and hydrophilic drugs. Moreover, SLNs are biocompatible and easy to sterilize. The used fabrication methods do not require organic solvents which may affect the toxicity of the final product. Finally, functionalization of the SLNs with specifically modified targeting lipids allows them to actively target desired tissues¹¹⁵. The common nanomaterials of SLNs are biodegradable, which consist of lipids that are physiologically compatible such as fatty acids, glycerides, sterols, etc. Therefore, based on nanotoxicological classification system (NCS), SLNs is generally considered as a groups of NCS classes I or III¹¹⁶.

SLNs have been extensively used for the delivery of the therapeutic drug into the CNS. SLNs have the potential to transport and release drugs to the brain because their particle size allows them to use the neuronal transport in the olfactory and trigeminal nerve¹¹⁷. In addition, the lipophilic nature of SLNs allows

these particles to pass BBB. Drug release from the matrix of nanoparticles occurs via two main mechanisms: (1) drug diffusion and (2) lipid degradation by enzymes (e.g., lipase, colipase)¹¹⁸. Several studies have shown the effectiveness of SLNs formulation using intranasal administration for several drug compounds that act on the central nervous system, including risperidone³⁰, haloperidol²⁹ and donepezil²⁸. Therefore, in this study, the solid lipid nanoparticles (SLNs) of AA have been developed for intranasal delivery to increase its availability in the brain.



CHAPTER 3

MATERIALS AND METHODS

3.1 Materials

3.1.1 Chemicals and Reagents

1,1,3,3-tetraethoxypropane (Sigma-Aldrich St. Louis, MO, USA)

Acetic acid glacial (Millipore, Billerica, MA, USA)

Acrylamide/Bisphosphate (Bio-Rad, laboratories, CA, USA)

Ammonium persulfate (Bio-Rad, laboratories, CA, USA)

Amyloid-Beta₁₋₄₂ (Sigma-Aldrich St. Louis, MO, USA)

Anti-rabbit Amyloid Beta₁₋₄₂ polyclonal antibody (Sigma-Aldrich St. Louis, MO, USA)

Anti-rabbit pTau S396 monoclonal antibody (Abcam, Cambridge, MA, USA)

Anti-rabbit pTau T231 monoclonal antibody (Abcam, Cambridge, MA, USA)

Anti-mouse Tau 5 monoclonal antibody (Abcam, Cambridge, MA, USA)

Anti-GAPDH antibody (Millipore, Billerica, MA, USA)

Anti-GFAP antibody (Abcam, Cambridge, MA, USA)

Anti-TMEM119 antibody (Abcam, Cambridge, MA, USA)

Alexa Fluor 568 anti-mouse (Life Technologies, OR, USA)

Alexa Fluor 488 anti-rabbit (Life Technologies, OR, USA)

Asiatic acid (Sigma–Aldrich St. Louis, MO, USA)

BCA protein assay kit (Thermo Scientific, Rockford, IL, USA)

Butanol (Sigma–Aldrich St. Louis, MO, USA)

Carboxymethylcellulose (Sigma–Aldrich St. Louis, MO, USA)

Chemiluminescence reagent (Millipore, Billerica, MA, USA)

Donepezil (Sigma–Aldrich St. Louis, MO, USA)

Glycine (Millipore, Billerica, MA, USA)

Horseradish peroxidase (HRP)-conjugated anti-rabbit (Millipore, Billerica, MA, USA)

Horseradish peroxidase (HRP)-conjugated anti-mouse (Millipore, Billerica, MA, USA)

IL-1Beta assay kit (Biolegend, CA, USA)

Non-Fat Dry Milk (Cell signalling Technology, Inc. USA)

Phenylmethylsulphonyl fluoride (PMSF) (Sigma–Aldrich St. Louis, MO, USA)

Polyvinylidene difluoride transfer membrane (Immobilon, Bedford, MA, USA)

Protein ladder (BLUE stainttm, Gold Biotechnology, Inc. US)

Pyridine (Sigma–Aldrich St. Louis, MO, USA)

Sodium chloride (Sigma–Aldrich St. Louis, MO, USA)

Sodium hydroxide (Merck, Darmstadt FR, Germany)

Sodium dodecyl sulfate (Millipore, Billerica, MA, USA)

Tetramethyl ethylenediamine (Millipore, Billerica, MA, USA)

Thiobarbituric acid (Sigma–Aldrich St. Louis, MO, USA)

TNF-Alpha assay kit (Biolegend, CA, USA)

Tris (Millipore, Billerica, MA, USA)

Tween-20 (Millipore, Billerica, MA, USA)

3.1.2 Equipments

Centrifuge (LEGEND MICRO 21R, Thermo Scientific, Rockford, IL, USA)

CG842 laboratory pH meter (SCHOTT® Instruments GmbH, Germany)

Confocal Microscope (ZEISS, LSM 900, Germany)

Cryostat microtome (Leica CM1950 Cyrostat, Leica Biosystems)

Dounce homogenizer (Glas-Col®, USA)

Luminescent image detector (ImageQuant™ LAS 4000, GE Healthcare Bio-sciences, Japan)

Microplate reader (CLARIOstar®, BMG LABTECH, Germany)

PG 2002-S Analytical balance (Mettler Toledo, Columbus, OH, USA)

Power supply (PowerPac, USA)

Temperature controlled water bath (Mettmert, Germany)

Trans-Blot SD semi-dry electrophoretic transfer cell (Trans-Blot®, USA)

VideoMOT2 system (TSE Systems, Germany)

VM300 Vortex mixer (Axiom®, Scientific Industries, Germany)

3.1.3 Drug Preparation

Asiatic Acid in SLNs (22.6 mg/10 mL) was prepared by Miss Tissana Rojanaratha and Prof. Garmpimol, Ph.D. from Department of Pharmaceutics and Industrial Pharmacy, Faculty of Pharmaceutical Sciences, Chulalongkorn University. In this study, 30 μ L of AA in SLNs was administered intranasally per one mouse per day. The average dose of AA was 2.04 ± 0.16 mg/kg/day. For oral administration, AA was suspended in 0.5% carboxymethylcellulose (CMC) in the concentrations of 0.3 and 3 mg/mL. Donepezil was dissolved in normal saline solution (NSS) in the concentration of 3 mg/mL.

3.1.4 Preparation of Amyloid-Beta₁₋₄₂ oligomers

A β ₁₋₄₂ oligomers were made as the previously described method^{119,120}. According to the manufacturer instruction, the monomer of A β ₁₋₄₂ can be dissolved in DMSO (Sigma–Aldrich St. Louis, MO, USA). In this study, A β ₁₋₄₂ monomer was dissolved in 10% DMSO in NSS to a final concentration of 0.22 nmol/ μ L. Before injected into mice brain, A β ₁₋₄₂ monomer was incubated at 37°C for 96 hr for aggregation process. The A β ₁₋₄₂ oligomers were confirmed by observation under light microscope as shown in Figure 2.

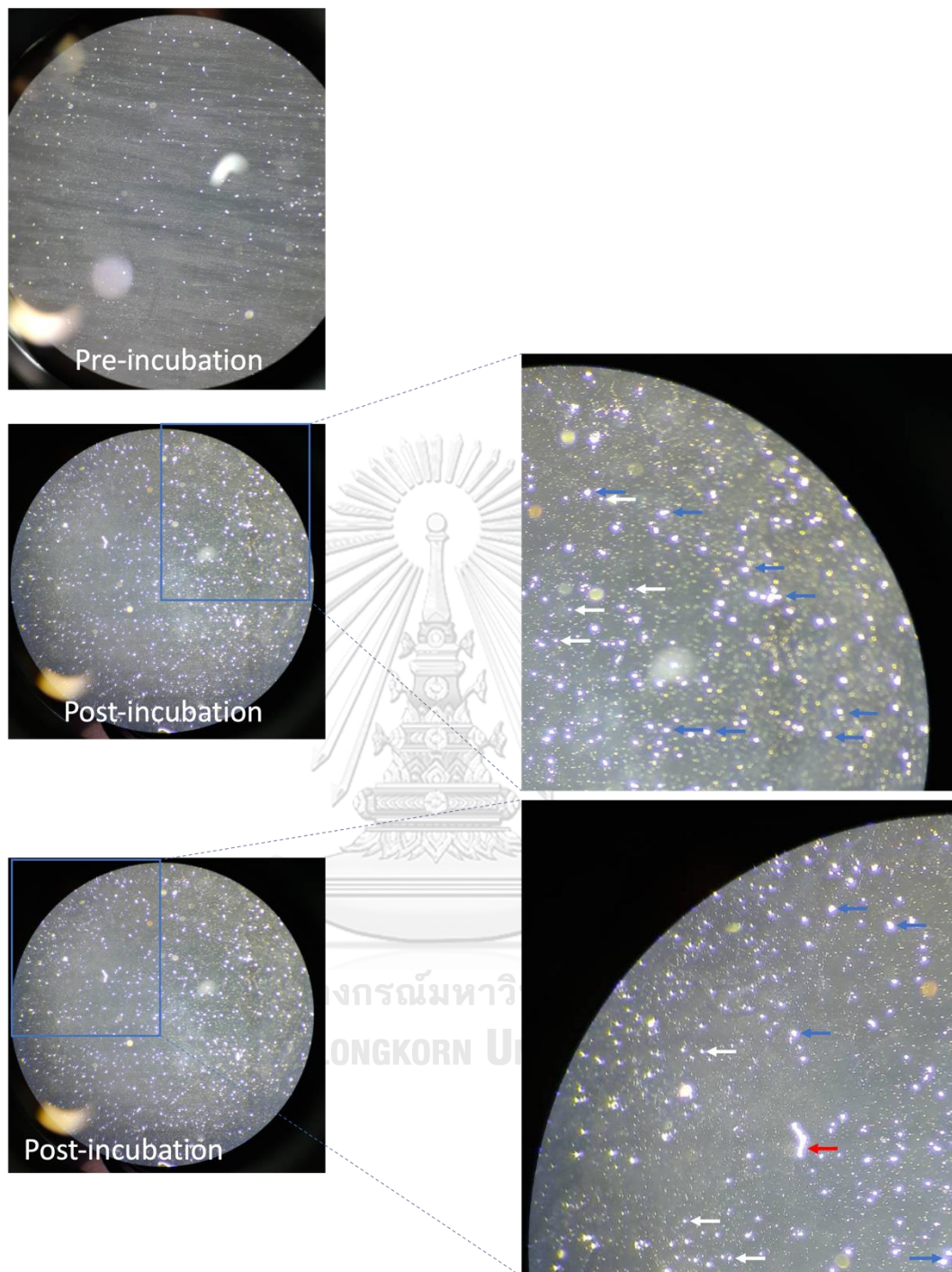


Figure 2 $A\beta_{1-42}$ fragments before and after 96-hr incubation at 37°C.

The monomer (white arrow), oligomer (blue arrow) and fibril (red arrow) forms of $A\beta_{1-42}$ were observed under light microscope.

3.1.5 Animals

Eight weeks-old male ICR mice, weighing 25-30 g, were obtained from Nomura Siam International, Bangkok, Thailand. The housing conditions were $22\pm 2^{\circ}\text{C}$, 40-60% humidity and a 12-hr light-dark cycle (light on at 7.00 A.M.). Mice were free to access food and water. Mice were allowed to acclimatize at least 7 days before the test. The animal experiment procedure was approved by the Institutional Animal Care and Use Commission, Faculty of Pharmaceutical Sciences, Chulalongkorn University (approval no. 21-33-002).

3.2 Methods

3.2.1 Experimental design

Neuroprotective effect of AA in SLNs by intranasal was conducted by *in vivo* study. All animals were evaluated for several behaviour tests related to the motoric function, anxiety-like behaviour and memory as illustrated in figure 3. At the end of study, brain tissues were used to determine the neuroprotective mechanisms.

A complete randomized design experiment was applied in this study. Mice were randomly divided into 6 groups (n=12 per group) and received treatment as indicated in table 2. All animals were allowed to acclimatize

for 1 week. Then, animals in group 4 were trained for intranasal administration technique using NSS for 7 days before i.c.v. injection. Mice in group 1 received NSS contained 10% DMSO (3 μ L) i.c.v. injection, while mice in groups 2-6 receive $A\beta_{1-42}$ (3 μ L) i.c.v. injection. Mice in group 1-2 received 0.5% CMC (10 mL/kg, p.o.) once daily for 28 days. Mice in group 3 received NSS 0.9% for 21 days followed by donepezil (3 mg/kg, p.o.) for 7 days during days 19-20 and days 23-27. Mice in group 4 received AA (average dose: 2.04 ± 0.16 mg/kg) via intranasal administration once daily for 28 days. Generally, intranasal doses are 2-10 times lower than oral doses¹²¹. Another study was also proposed that the dosage to be delivered via nasal administration can be as low as 0.01–1% of oral dosage¹⁰⁵. AA in SLNs was administered to each mouse in awaken state at the maximal volume 30 μ L, 15 μ L each nostril. Mice in group 5 and 6 received AA via gavaging once daily for 28 days at the dose 3 and 30 mg/kg, respectively.

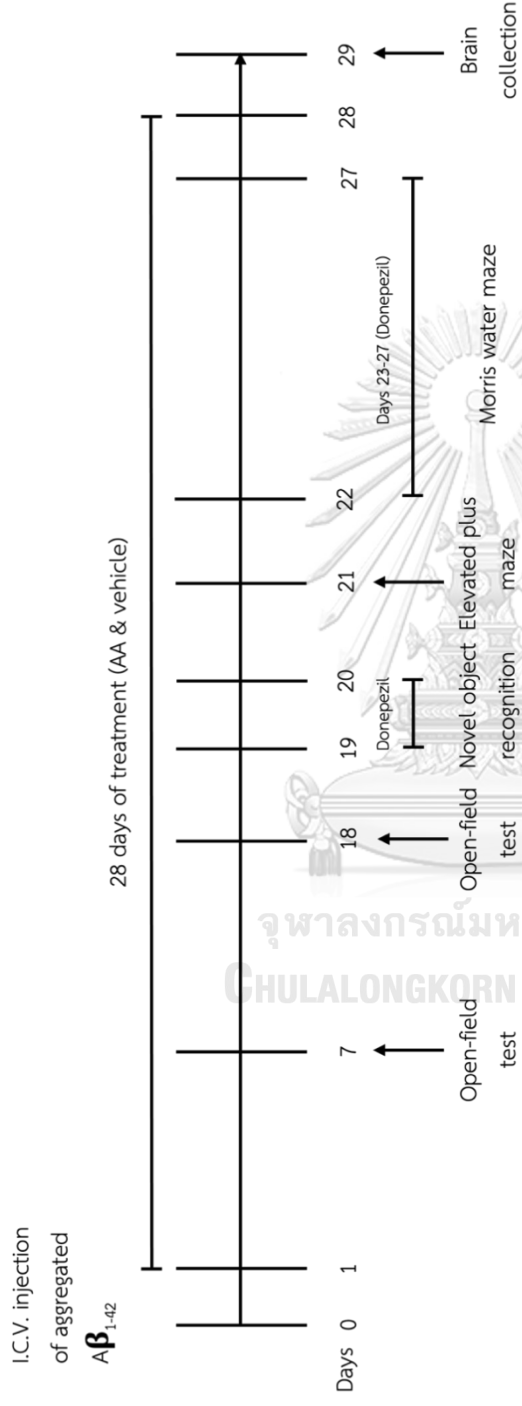


Figure 3 Experimental timeline of the neuroprotective effect of AA

Table 2 Animal group and the treatment

No	Group	i.c.v. injection	Treatment	Duration of treatment	Time
1	Sham	10% DMSO in NSS (3 μ L)	0.5% CMC-Na (10 mL/kg, p.o.)	28 Days	Day 1-28
2	AD	A β ₁₋₄₂ (3 μ L)	0.5% CMC-Na (10 mL/kg, p.o.)	28 Days	Day 1-28
3	AD-DON	A β ₁₋₄₂ (3 μ L)	NSS 0.9% (10 mL/kg, p.o.) Donepezil (3 mg/kg, p.o.)	21 Days 7 Days	Day 1-18, Day 21-22, Day 28 Day 19-20, Day 23-27
4	AD-INAA	A β ₁₋₄₂ (3 μ L)	Asiatic acid (2.04 \pm 0.16 mg/kg, i.n.)	28 Days	Day 1-28
5	AD-POAA3	A β ₁₋₄₂ (3 μ L)	Asiatic acid (3 mg/kg, p.o.)	28 Days	Day 1-28
6	AD-POAA30	A β ₁₋₄₂ (3 μ L)	Asiatic acid (30 mg/kg, p.o.)	28 Days	Day 1-28

3.2.2 Intracerebroventricular Injection of Amyloid Beta₁₋₄₂

Mice were injected with A β ₁₋₄₂ into the brain lateral ventricle to induce neurotoxicity and memory impairment¹²⁰. Mice were anesthetized with isoflurane. The depth of anaesthesia level was monitored by foot pinch. Direct i.c.v. injection was conducted by using a modified insulin syringe. The length of the needle was adjusted with parafilm to 3.8 mm to enable the accuracy of the depth injection according to the DV coordinate of the lateral ventricle (-2.4 mm at bregma) and the skull thickness. As shown in figure 4, the blue star is indicated the coordinate target that is

within the range of lateral ventricle at the coordinate of AP = -0.2 to -0.5 mm and ML = +0.7 to +1.1 mm from the bregma.

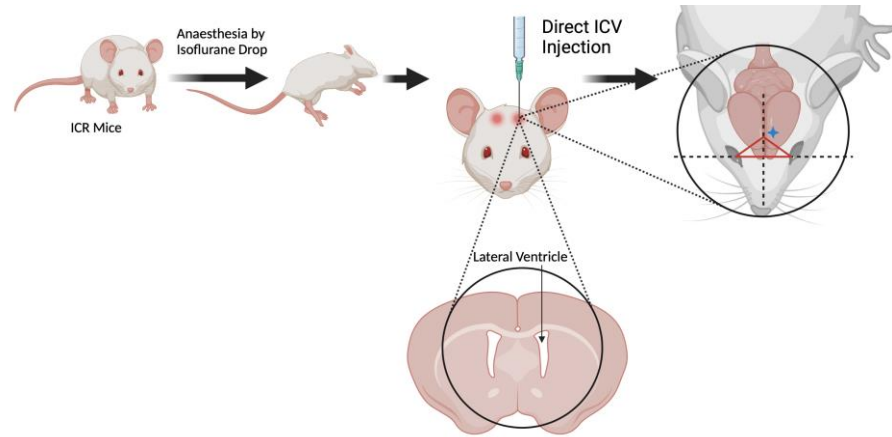


Figure 4 The direct intracerebroventricular (i.c.v.) injection of $A\beta_{1-42}$

3.2.3 Behavioural Tests

3.2.3.1 Open-Field Test (OFT)

Exploration activity was measured in the open-field test on experimental days 7 and 18. Sixty minutes after treatment, mice were allowed to walk freely in the black box (50 x 50 x 40 cm) for 5 minutes. The video tracking set was placed over the box and connected to VideoMOT2 software for real-time analysis of locomotor activity. The exploration time (second) and exploration distance (cm) were measured. On day 18, the additional parameters, time spent in the center zone (second), the number of center visit and distance in the center zone (cm), were added to

evaluate the anxiety level. The exploration evaluation on day 18 was also set as the habituation day before the novel object recognition test (NORT) on day 19-20.

3.2.3.2 Novel Object Recognition Test (NORT)

On days 19-20, mice performed the novel object recognition task to determine their recognition memory (figure 5). NORT was performed 60 minutes of treatment. In the familiarisation phase, each mouse was placed in the black box (50 x 50 x 40 cm) box containing two identical objects. The mouse was allowed to explore the objects for 10 minutes. The second familiarization phase was conducted again on day 20 for 10 minutes. Then, the mouse was returned to its home cage for 2 hr. In the test phase, one of the objects was changed to a novel object. The mice were allowed to explore the novel and familiar objects for 5 minutes. Time spent exploring the objects during the familiarisation and test phases were recorded and analysed manually by a blinded experimenter. Discrimination index was calculated as the exploration time on the novel object minus the exploration time on the familiar object then divided by the total exploration time on

both objects. Percentage preference index was calculated as the exploration time on the novel object divided by the total exploration time on both objects then multiplied by 100.

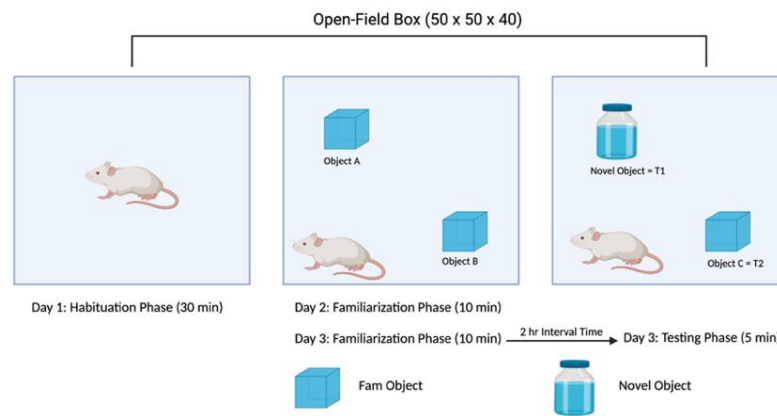


Figure 5 Experimental design for novel object recognition test

3.2.3.3 Elevated Plus Maze (EPM)

On day 21, mice were performed the elevated plus maze (EPM) test to determine anti-anxiety effects of the treatment. The elevated plus-maze apparatus consisted of two open arms with no wall (30 cm length, 5 cm width), two enclosed arms with a black wall (30 cm length, 5 cm width, 16 cm height of the wall) and a central platform (5 x 5 cm). The maze was elevated 40 cm above the floor. Sixty minutes after treatment, mouse was placed at the centre of the maze, facing one of the open arms and allowed to freely explore the maze for 5 minutes. The following parameters

were recorded: (1) time spent in open arms, (2) time spent in enclosed arms, (3) number of open arm entries, and (4) number of enclosed arm entries. The video tracking set was placed over the apparatus and connected to VideoMOT2 software for real-time analysis of those parameters.

3.2.3.4 Morris Water Maze (MWM)

Morris water maze was used to evaluate the learning and spatial memory in animals. The maze consisted of a circular pool (150 cm diameter, 40 cm height) filled with water ($22\pm 2^{\circ}\text{C}$) and a platform. A circular pool was divided into 4 quadrants (Q1-Q4) in VideoMOT2. A platform was fixed in the middle of Q4 (figure 6). Four different visual cues were put on the wall of the pool. On day 22 (MWM day 0), the platform was visible (1 cm above water level), a mouse was put in the pool in each quadrant (Q1, Q2, Q3) (a total of 3 times/day) and allowed to find the platform for the 60s. If a mouse can find the platform, it was allowed to stay on the platform for the 30s. If a mouse cannot find the platform within the 60s (cut-off time), an experimenter will put that mouse on the platform and allowed it to stay for the 30s. The same procedure

was also performed on days 22-26 (MWM days 1-5) but the platform was hidden 1 cm underwater. Latency and swimming latency was recorded by VideoMOT2. On the probe trial day (experimental day 27, MWM day 6), the platform was removed. A mouse was placed in the pool of each quadrant (Q1, Q2, Q3) and allowed to swim for the 60s. Swimming time and distance travelled in the platform quadrant were recorded by VideoMOT2.

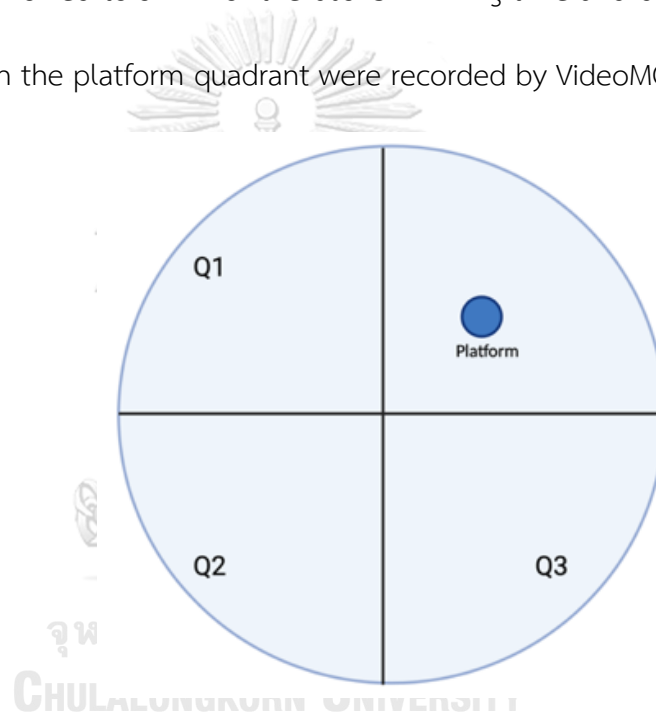


Figure 6 Diagram of a circular pool in Morris water maze

3.2.4 Brain Collection

Mice brains were collected 24 h after the last treatment (Day 29). Six mice per group were euthanized by cervical dislocation. Brains were quickly removed and snap-freeze in the liquid nitrogen and then kept at -80°C for further analysis. For histology study, mice were euthanized by CO₂

and transcardially perfused with cold-PBS followed by 4% paraformaldehyde (PFA) and kept at 4°C until further analysis.

3.2.5 Western Blot Analysis

Western blot was used to evaluate the expression of tau hyperphosphorylation in the prefrontal cortex and hippocampus tissues. Each tissue was homogenized with lysis buffer consisting of RIPA buffer, 1 mM phenylmethylsulphonyl fluoride (PMSF), NP-40, Triton-X 100 and protease inhibitor. Homogenates were then centrifuged at 16,000 g for 20 min at 4°C. The collected supernatant was used for western blot analysis. The total protein concentration was determined using a BCA protein assay kit. The protein concentration was adjusted to 10 μg and 60 μg for pTau and Tau, respectively using a loading buffer. Protein samples were denatured at 95°C for 5 min followed by electrophoresis in 10% SDS-PAGE gel at 80 V for 3 h. Then, protein was transferred onto a PVDF membrane at 9 V for 1.5 h. For blocking unspecific proteins, the membrane was incubated with 5% non-fat dry milk (NFDM) for pTau protein and 3% skim milk for Tau 5 protein in Tris-buffered saline containing 0.1% Tween-20 (TBST) for 1 h at room temperature. Next, the membrane was incubated overnight at 4°C with the rabbit monoclonal anti-pTau S396

(1:1000), anti-pTau T231 (1:1000) and anti-Tau 5 (1:1000). After that, the membrane was incubated at room temperature for 2 h with a horseradish peroxidase (HRP)-conjugated goat anti-mouse IgG antibodies (1:1000) for Tau 5 and GAPDH protein and anti-rabbit IgG antibodies (1:1000) for pTau protein. A chemiluminescence reagent was used to develop the membrane and analyzed with a luminescent image detector (Image Quant LAS 4000, GE Healthcare Biosciences, Japan). The protein band density was measured by Image J software. All data were calculated as ratio to Sham as one after normalized with GAPDH.

3.2.6 Enzyme-linked Immunosorbent Assay (ELISA)

ELISA was used to evaluate the level of proinflammatory mediators, TNF- α and IL-1 β in the brain tissue excluding the prefrontal cortex, hippocampus and cerebellum. The measurement was conducted following the manufacturer's instructions (Biolegend, CA, USA). Firstly, the plate was coated with captured antibody followed by overnight incubation at 4 °C. Then, the plate was washed with a phosphate-buffered solution containing 0.05% Tween-20 (PBST) for 4 times. For blocking unspecific protein, assay diluent A was added to each well and incubated at room temperature with shaking for 1 h. After that, all samples and standards were added to

each well and shaken again for 2 h at room temperature. Next, all samples were incubated with the primary antibody for 1 h followed by incubation with the secondary antibody (the Avidin-HRP) for 30 min at room temperature. Then, incubate samples with TMB substrate for 15 min at room temperature to develop the blue colour of the positive well. Lastly, 2N H₂SO₄ was added to stop the reaction and the absorbance was read at 450 nm for 15 min. All data were provided as pg/mg protein.

3.2.7 Lipid Peroxidation Assay

Lipid peroxidation was evaluated using thiobarbituric acid reactive species (TBARS) method. 1,1,3,3-tetraethoxypropane (TEP) was used to make a standard curved. Brains were weighed and homogenized with ice-cold PBS (1:5 w/v PBS) at 4°C. Brain tissues were then centrifuged for 15 min at 2000 g. The total protein in the supernatant was determined by BCA kit. One hundred μ L of the supernatant was added with 1.5 mL of 20% acetic acid, 1.5 mL of 0.8% thiobarbituric acid (0.8%) and 0.2 mL of 8.1% sodium dodecyl sulphate (SDS) and incubated in the water bath at 95°C for 60 min. All samples were cooled down for 10 min after incubation. After that, 2 mL of butanol: pyridine (15:1 v/v) was added and centrifuged for 15 min at 2000 g. The collected supernatant was measured

using a microplate reader at 532 nm. The data was provided as mmol/mg protein.

3.2.8 Histology Analysis

Brain histology was used to analyse the expression of $A\beta_{1-42}$, glial cell markers and neuronal cell death in the brain tissue. Brains in 4% PFA were transferred into 10%, 20%, and 30% sucrose, respectively and incubated in 30% sucrose for at least 48 h. Then, brains were cut in 40 μm thickness by coronal sections using a cryostat at -20°C . The selection of brain area was following the bregma coordinates that represent hippocampus including CA1 and CA3 subregion.

3.2.8.1 Immunohistochemistry

For amyloid-beta₁₋₄₂ distribution, the selected sections were incubated with 1% of H_2O_2 for 30 min and transferred to 5% BSA for 1 h to block unspecific protein. Then, the sections were labelled with the primary antibody anti- $A\beta_{1-42}$ polyclonal antibody AB5078P (1:1000) at 4°C overnight followed by a 2-h incubation with the secondary antibody biotin-conjugated anti-goat antibody

(1:500). The complexes were trapped with the Avidin-Biotin complex (Vector, CA, USA) followed by reacting with 3,3'-diaminobenzidine (Wako, Japan). The $A\beta_{1-42}$ oligomers were analysed qualitatively to confirm the present of $A\beta_{1-42}$ oligomers in the hippocampus region at the bregma -1.55 until -2.69 mm. $A\beta_{1-42}$ detection in mice hippocampus was shown in Figure 7.

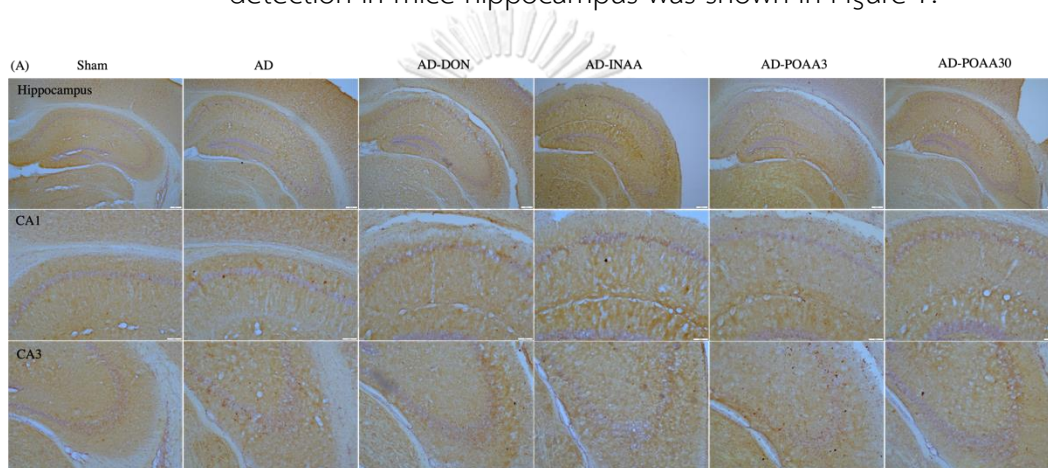


Figure 7 Distribution profile of $A\beta_{1-42}$ in the hippocampus of mice.

3.2.8.2 Immunofluorescence

In the immunofluorescence staining, the selected sections were transferred into the frosted-adhesive slide glass and air-dried overnight. Sections were blocked with 1% BSA in PBS containing 0.5% triton-X and 0.3 M glycine at room temperature for 1 h, then subsequently incubated with the mouse monoclonal anti-GFAP (1:500) and the rabbit monoclonal anti-TMEM119 (1:500) at 4°C

overnight. After that, the section was incubated at room temperature for 2 h with goat anti-mouse IgG antibodies Alexa Fluor 586 (red, 1:1000) and goat anti-rabbit IgG antibodies Alexa Fluor 488 (green, 1:1000). Then, nuclear DNA was labelled with DAPI (blue). The staining was observed under the confocal microscope. The specimen was automatically detected by artificial intelligent (AI) sample finder in the system. To produce the immunofluorescence signal, several parameters including airy units, laser percentage, and master gain were set as 1, 10-20%, and 700-800 V, respectively. Then, appropriate live imaging of each signal was snapped and merged by the system. The percentage of area covered by either astrocytes or microglia were measured by Image J software over the threshold. The threshold was set to determine appropriate immunolabelled area (signal) and minimize unspecific signal attributable in the immunolabelling process (noise). The threshold was manually defined by comparing the real area of signal with the area produced by ImageJ software. At last, the same threshold range of 25-255 were applied to images from all experimental groups. The bregma coordinate were -1.55 until -2.69 mm.

3.2.8.3 Nissl Staining

The survival neurons in the hippocampus were confirmed by the Nissl staining procedure. The selected section (five sections per animal from bregma -1.79 to -2.45 mm) was transferred to a glass slide and air-dry for 10 min. The sections were dehydrated in ethanol and impregnated with the cresyl violet acetate as shown in table 3. Then, the section was mounted using mounting media and closed with a cover slide. The number of neurons in CA1 and CA3 was counted individually by the blinded experimenter.

Table 3 Nissl staining step-by-step protocol.

Step No.	Reagent	Time incubation
1	Ethanol absolute	3 min (twice)
2	Ethanol 95%	3 min (twice)
3	Ethanol 70%	3 min (once)
4	Ethanol 50%	3 min (once)
5	Cresyl violet 0.1%	1 min (once)
6	DI water	1 min (once)
7	Ethanol 70%	3 min (once)
8	Ethanol 95%	3 min (once)
9	Ethanol absolute	3 min (once)
10	Xylene	3 min (twice)

3.3 Data Analysis

All data were expressed as mean + S.E.M. and analysed using Graphpad Prism version 8.0 (GraphPad Software, San Diego, CA, U.S.A.). The comparison of all parameters between all groups was determined by one-way analysis of variance (ANOVA) followed by Tukey's post-hoc test (HSD) except time spent in the target quadrant in probe trial which followed by LSD post-hoc test for multiple comparisons. Two-way ANOVA followed by Tukey's post-hoc test (HSD) was applied for parameters in Morris water maze including escape latency and swimming distance. The comparison between mean exploration time on the familiar and novel object in the testing phase of novel object recognition test was analysed by multiple paired *t*-test. All analyses with significance *p*-values < 0.05 represents statistical significance differences.

CHAPTER 4

RESULTS

4.1 The protective effect of nasal delivery and oral administration of AA against spatial memory dysfunction induced by A β ₁₋₄₂

Morris water maze was used to investigate the protective effect of nasal and oral administration of AA on spatial memory dysfunction. On the first day of the test, a visible platform was set to measure the baseline level. It was shown that the escape latency and the swimming distance were not significant different among the experimental groups. Two-way ANOVA showed effects of time and treatment on the escape latency and the swimming distance on days 2-5 (hidden platform) (time: (F (4, 325) = 22.60, p < 0.0001) and (F (4, 325) = 28.68, p < 0.0001), respectively; treatment: (F (5, 325) = 20.07, p < 0.0001) and (F (5, 325) = 28.80, p < 0.0001), respectively). Mice in the AD group exhibited significant longer escape latency and swimming distance on days 2-5 than mice in the Sham group (escape latency: p < 0.01, p < 0.01, p < 0.01 and p < 0.001, respectively; swimming distance: p < 0.001, p < 0.01, p < 0.001 and p < 0.001, respectively, Tukey's post-hoc test). Donepezil, as a positive control, significantly reduced the escape latency and the swimming distance of AD mice on days 2-5 compared to the AD group (escape latency: p < 0.01, p < 0.05, p < 0.001 and p < 0.01, respectively; swimming distance: p < 0.001, p < 0.01, p < 0.001 and p <

0.001, respectively, Tukey's post-hoc test). Similar to donepezil, the escape latency and the swimming distance of AD mice treated with AA in SLNs by nasal administration (AD-INAA) were significantly lower than that of the AD group on days 2-5 (escape latency: $p < 0.01$, $p < 0.05$, $p < 0.001$ and $p < 0.01$, respectively; swimming distance: $p < 0.001$, $p < 0.01$, $p < 0.001$ and $p < 0.001$, respectively, Tukey's post-hoc test), indicating that nasal delivery of AA in SLNs attenuated spatial learning and memory dysfunction induced by $A\beta_{1-42}$. Furthermore, high oral dose of AA significantly decreased the escape latency and the swimming distance of AD mice (AD-POAA30) on days 4 and 5 (escape latency: $p < 0.01$ and $p < 0.05$, respectively; swimming distance: $p < 0.001$ and $p < 0.001$, respectively, Tukey's post-hoc test). However, the treatment of low oral dose of AA in AD mice (AD-POAA3) failed to decrease the escape latency and the swimming distance compared to the AD group (Figure 8A, 8B).

Two-way ANOVA revealed showed no effect of treatment, time, and time x treatment interaction on swimming speed ($F(4, 325) = 2.04$, $p = 0.0890$, $F(5, 325) = 2.16$, $p = 0.0578$), and $F(20, 325) = 0.5149$, $p = 0.9600$, respectively), suggesting that motoric function did not alter the swimming ability of animals (Figure 8C). The tracking pathway of mice on the last day of learning phase (day 5) was shown in Figure 8D.

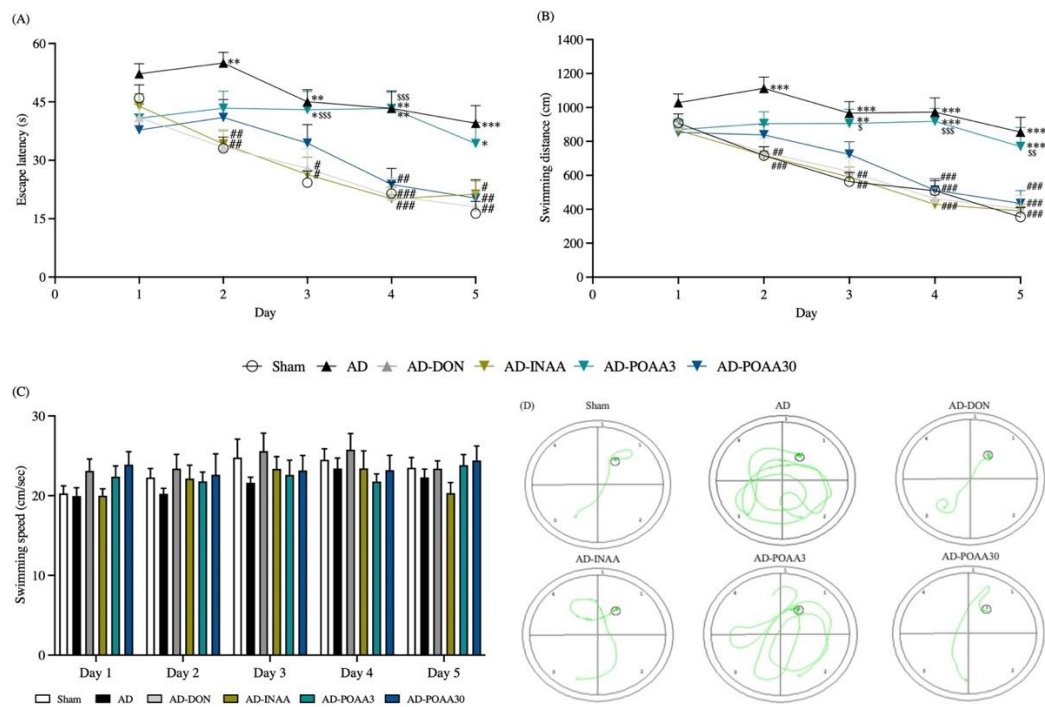


Figure 8 The effect of AA by intranasal and oral administration on the spatial memory dysfunction induced by $A\beta_{1-42}$ in the Morris water maze test

(A) Latency time to reach the platform, (B) swimming distance to reach the platform, (C) swimming speed during the Morris water maze, (D) representative of tracking pattern on day 5 of MWM. Data are expressed as mean + S.E.M. ($n = 11-12/\text{group}$), * $p < 0.05$, ** $p < 0.01$, *** $p < 0.001$ compared to Sham, # $p < 0.05$, ## $p < 0.01$, ### $p < 0.001$ compared to AD, \$ $p < 0.05$, \$\$ $p < 0.01$, \$\$\$ $p < 0.001$ compared to AD-INAA.

To evaluate long-term memory function, probe trial was performed one day after the last learning phase (Day 6). One-way ANOVA revealed the effect of treatments on the time spent in the target quadrant ($F(5, 64) = 2.022$, $p < 0.0873$). AD mice significantly decreased time spent in the target quadrant compared to the Sham group ($p < 0.05$, Fisher's LSD post-hoc test). AD mice that treated with donepezil (AD-DON), AA in SLNs (AD-INAA), high oral dose of AA (AD-POAA30) caused

a significant increase in the time spent in the target quadrant compared to the AD group ($p < 0.05$, $p < 0.05$ and $p < 0.01$, respectively, Fisher's LSD post-hoc test) (Figure 9A). However, the time spent in the target quadrant of AD mice treated with low oral dose of AA (AD-POAA3) was not significantly different compared to the AD group ($p = 0.2366$, Fisher's LSD post-hoc test). The swimming speed in the probe trial was also not significant different among groups (Figure 9B).

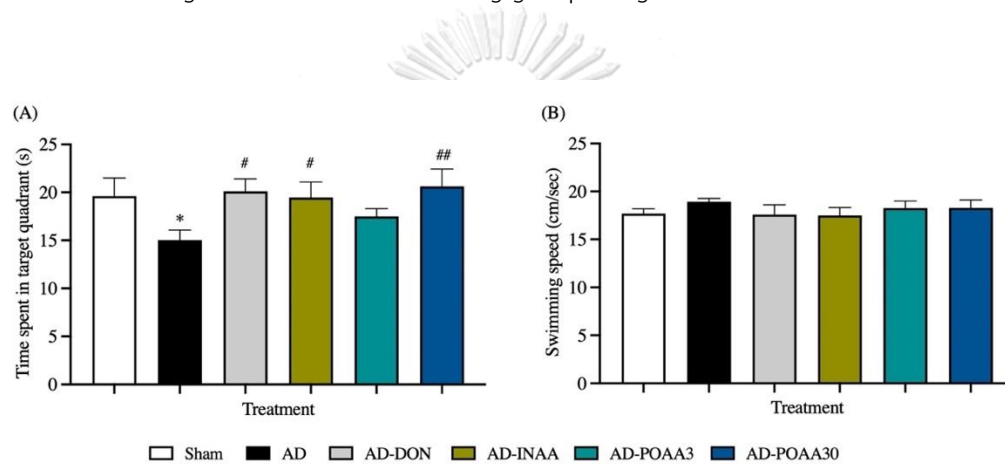


Figure 9 The effect of AA by intranasal and oral administration on the long-term memory dysfunction induced by $A\beta_{1-42}$ in the Morris water maze test (A) Time spent in the target quadrant and (B) swimming speed in the target quadrant during the probe trial in the Morris water maze. Data are expressed as mean + S.E.M. ($n = 11-12$ /group), * $p < 0.05$ compared to Sham, # $p < 0.05$, ## $p < 0.01$ compared to AD.

4.2 The protective effect of nasal delivery and oral administration of AA against recognition memory dysfunction induced by A β ₁₋₄₂

Novel object recognition test (NORT) was used to investigate the recognition memory in mice. In the testing phase, the mean exploration time on the novel object of mice in the Sham group was significantly higher than that on the familiar object ($p < 0.0001$, paired t -test), while the mean exploration time in the AD group showed no significant difference between novel and familiar object ($p = 0.938678$, paired t -test). Donepezil, INAA, and POAA30 treatments increased the mean exploration time on the novel object significantly compared to the familiar object ($p < 0.0001$, $p < 0.05$ and $p < 0.001$, respectively, paired t -test). In contrast, the mean exploration time between the novel and familiar object was not significantly different in AD mice treated with POAA3 ($p = 0.135879$, paired t -test) (Figure 10A).

One-way ANOVA revealed the effect of treatments on the discrimination index and preference index in the NOR test ($F(5, 57) = 5.646$, $p = 0.0003$ and $F(5, 57) = 5.617$, $p = 0.0003$, respectively). The discrimination index and preference index of AD mice group were decreased significantly compared to mice in the Sham group ($p < 0.001$ and $p < 0.001$, respectively, Tukey's post-hoc test). Donepezil, INAA and POAA30 treatments increased the discrimination index and preference index significantly compared to AD group (donepezil: $p < 0.01$ and $p < 0.01$, respectively; INAA: $p < 0.05$ and $p < 0.05$, respectively; POAA30: $p < 0.05$ and $p < 0.05$, respectively, Tukey's post-hoc test). In opposite, the discrimination index and

preference index of AD-POAA3 group were lower significantly compared to the Sham group ($p < 0.05$ and $p < 0.05$, respectively, Tukey's post-hoc test) (Figure 10B, 10C). There was no significant different on the total exploration time in the testing phase among groups (Figure 10D).



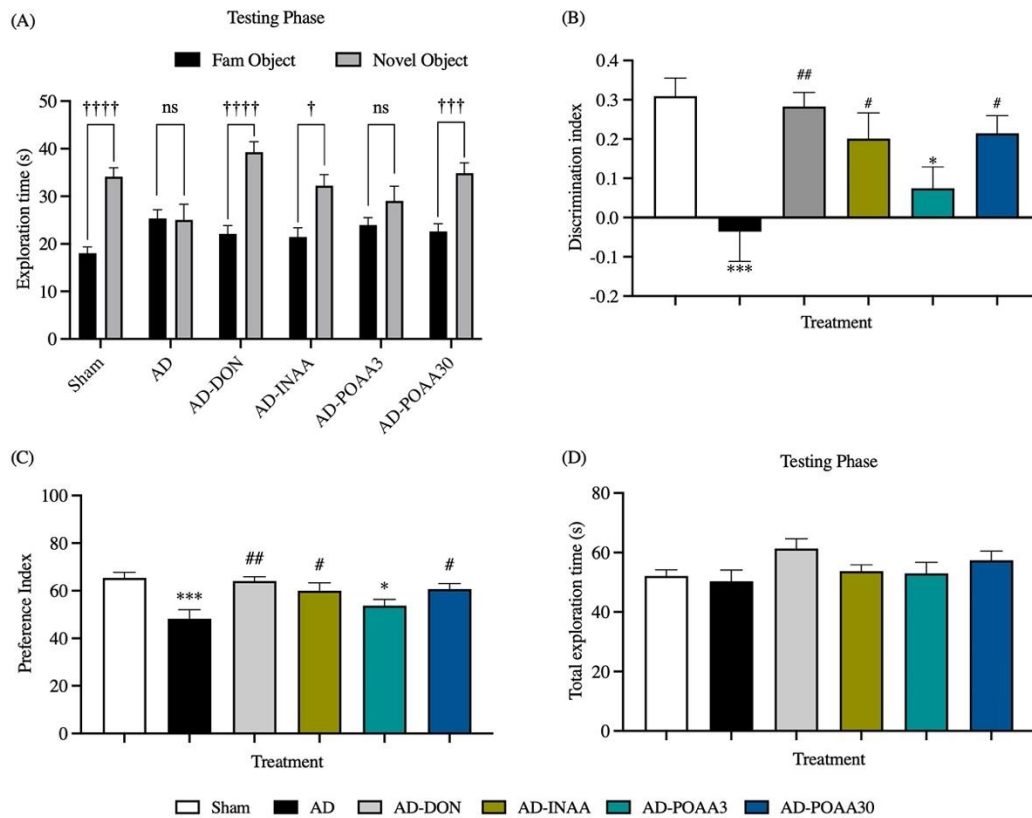
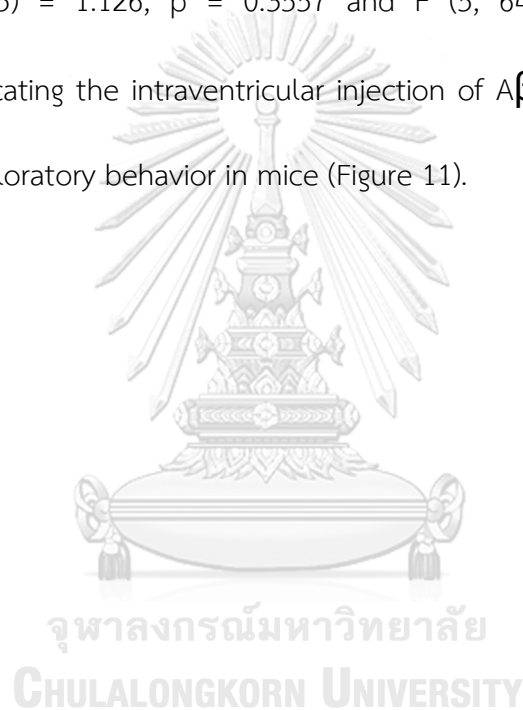


Figure 10 The effect of AA by intranasal and oral administration on the recognition memory impairment induced by $A\beta_{1-42}$ in the novel object recognition test (A) Exploration time in the testing phase, (B) discrimination index, (C) preference index, (D) total exploration time in the testing phase. Data are expressed as mean + S.E.M. (n = 10-11/group). †p < 0.05, ††p < 0.001, †††p < 0.0001 novel object vs familiar object, *p < 0.05, ***p < 0.001 compared to Sham, #p < 0.05, ##p < 0.01 compared to AD, ns = not significant.

4.3 The effect of $A\beta_{1-42}$ and AA on exploratory behaviour in mice

On day 7 and 18, exploration activity was evaluated to determine the motor function after the injection of $A\beta_{1-42}$ and the treatment. One way ANOVA revealed no effect of treatment on locomotion time and distance on days 7 and 18 (locomotion time: $F(5, 65) = 1.370$, $p = 0.2472$ and $F(5, 65) = 1.312$, $p = 0.2698$, respectively; distance: $F(5, 65) = 1.126$, $p = 0.3557$ and $F(5, 64) = 0.8479$, $p = 0.5210$, respectively), indicating the intraventricular injection of $A\beta_{1-42}$ and AA treatment did not affect the exploratory behavior in mice (Figure 11).



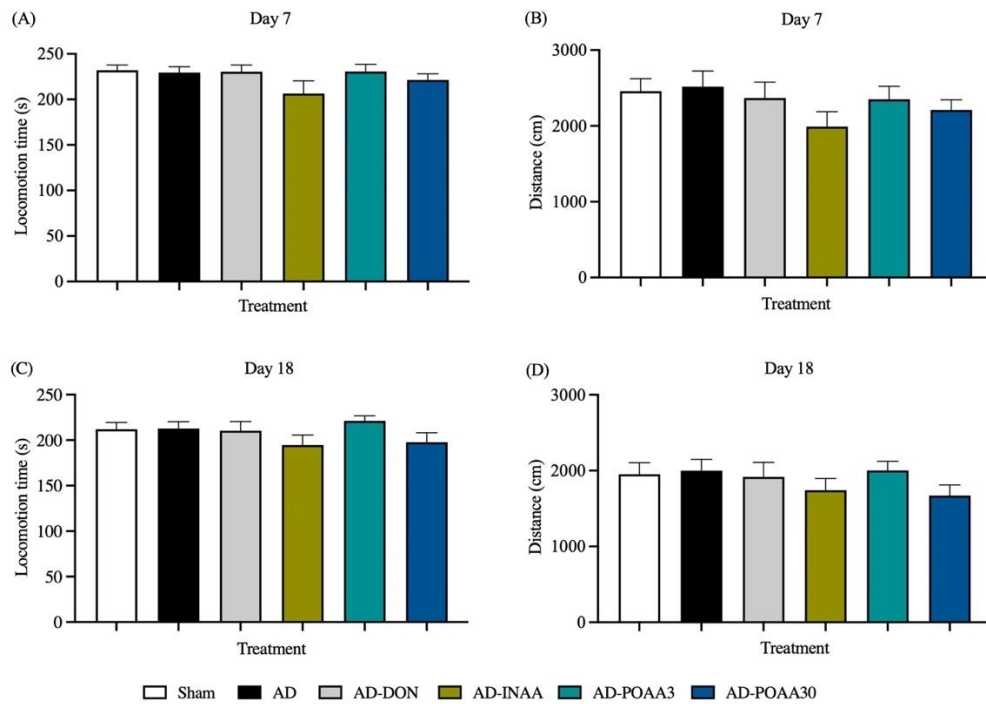


Figure 11 The effect of $A\beta_{1-42}$ and AA treatment on exploration activity in the open-field test

(A) Locomotion time and (B) distance on day 7, (C) locomotion time and (D) distance on day 18. Data are expressed as mean + S.E.M. (n = 11-12/group).

4.4 The effect of $A\beta_{1-42}$ and AA on the anxiety-like behaviour in mice

Anxiety-like behaviour was evaluated by open-field test on day 18 and elevated plus maze test on day 21. Donepezil was not given in the AD-DON group during this evaluation. One-way ANOVA revealed that all parameters in the open field apparatus including number of center visit ($F(4, 52) = 0.5724, p = 0.6838$), time spent in the center zone ($F(4, 54) = 1.601, p = 0.1875$), and distance in center zone ($F(4, 54) = 0.5086, p = 0.7296$) were not significantly different between experimental groups (Figure 12A, 12B, 12C). In line with the results in the elevated plus maze test, one-way ANOVA revealed no significant difference among experimental groups in the anxiety-like behaviour parameters which were the number of open arms visit ($F(4, 55) = 2.005, p = 0.1066$) (Figure 12D), the time spent in the open arms ($F(4, 54) = 0.9959, p = 0.4178$) (Figure 12E) and closed arms ($F(4, 55) = 0.5197, p = 0.7215$) (Figure 12H) and the distance in the open arms ($F(4, 54) = 1.554, p = 0.1997$) (Figure 12F) and closed arms ($F(4, 55) = 0.9192, p = 0.4594$) (Figure 12I). However, one-way ANOVA revealed the effect of treatment on the number of closed arms visit ($F(4, 53) = 4.767, p = 0.0023$) (Figure 12G.). The number of closed arms visit in the AD group was significantly higher than that on the Sham group ($p < 0.05$, Tukey's post-hoc test). Meanwhile, INAA treatment was significantly reduced the number of closed arms visits compared to mice in the AD group ($p < 0.05$, Tukey's post-hoc test). The number of closed arms visit of AD-POAA3 mice was also higher significantly compared to the AD-INAA group ($p < 0.05$, Tukey's post-hoc test). Therefore, our

results suggested that either $A\beta_{1-42}$ or AA treatment did not modulate anxiety-like behaviour in ICR mice.

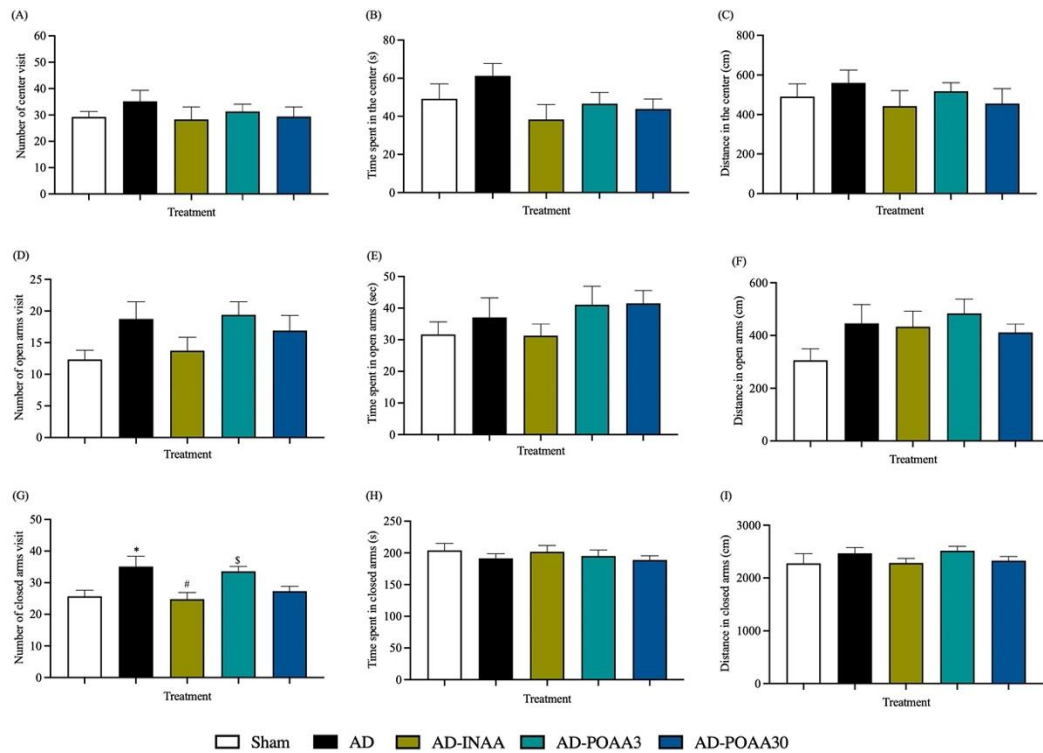


Figure 12 The effect of $A\beta_{1-42}$ and AA treatment on the anxiety-like behavior (A) Total number of center visit, (B) Time spent in the center zone, and (C) Distance in the center zone in the open-field test on Day 18. (D) Total number of open arms visits, (E) Time spent in the open arms and (F) Distance in the open arms in the elevated-plus maze. (G) Total number of closed arms visits, (H) Time spent in the closed arms and (I) Distance in the closed arms in the elevated-plus maze. Data are expressed as mean + S.E.M. (n = 10-12/group). * $p < 0.05$ compared to Sham; # $p < 0.05$ compared to AD; \$ $p < 0.05$ compared to AD-INAA.

4.5 The protective effect of nasal delivery and oral administration of AA against tau hyperphosphorylation induced by A β ₁₋₄₂

The expression of hyperphosphorylated tau and total tau protein in the hippocampus and prefrontal cortex were measured using western blot technique. One-way ANOVA reported the effect of treatment on the expression levels of pTau S396 and pTau T231 in mice hippocampus (F (5, 28) = 7.512, p = 0.0001 and F (5, 29) = 6.552, p = 0.0003, respectively). In the hippocampus, pTau S396 and pTau T231 expression levels of AD mice were significantly higher than that of the Sham group (p < 0.01 and p < 0.01, respectively, Tukey's post-hoc test). INAA and POAA30 treatments significantly decreased pTau S396 and pTau T231 expression levels in the hippocampus compared to the AD group (INAA: p < 0.05 and p < 0.01, respectively; POAA30: p < 0.05 and p < 0.001, respectively, Tukey's post-hoc test) (Figure 13A, 13B). The expression level of pTau S396 in the hippocampus of AD-POAA3 mice was significantly higher than that of mice in the Sham and AD-INAA group (p < 0.001 and p < 0.01, respectively, Tukey's post-hoc test).

In the prefrontal cortex, pTau S396 and pTau T231 expression levels were not significantly different among groups (F (5, 29) = 0.6905, p = 0.6346 and F (5, 29) = 2.570, p = 0.0483, respectively). However, the expression of pTau S396 and pTau T231 of AD mice slightly increased compared to the Sham group in the prefrontal cortex (Figure 13C, 13D). Tau 5 (as total tau) expression was not significant different among groups in the hippocampus and prefrontal cortex (F (5, 28) = 0.4768, p =

0.7904 and $F(5, 29) = 0.2102$, $p = 0.9555$, respectively, one way ANOVA) (Figure 13E, 13F).



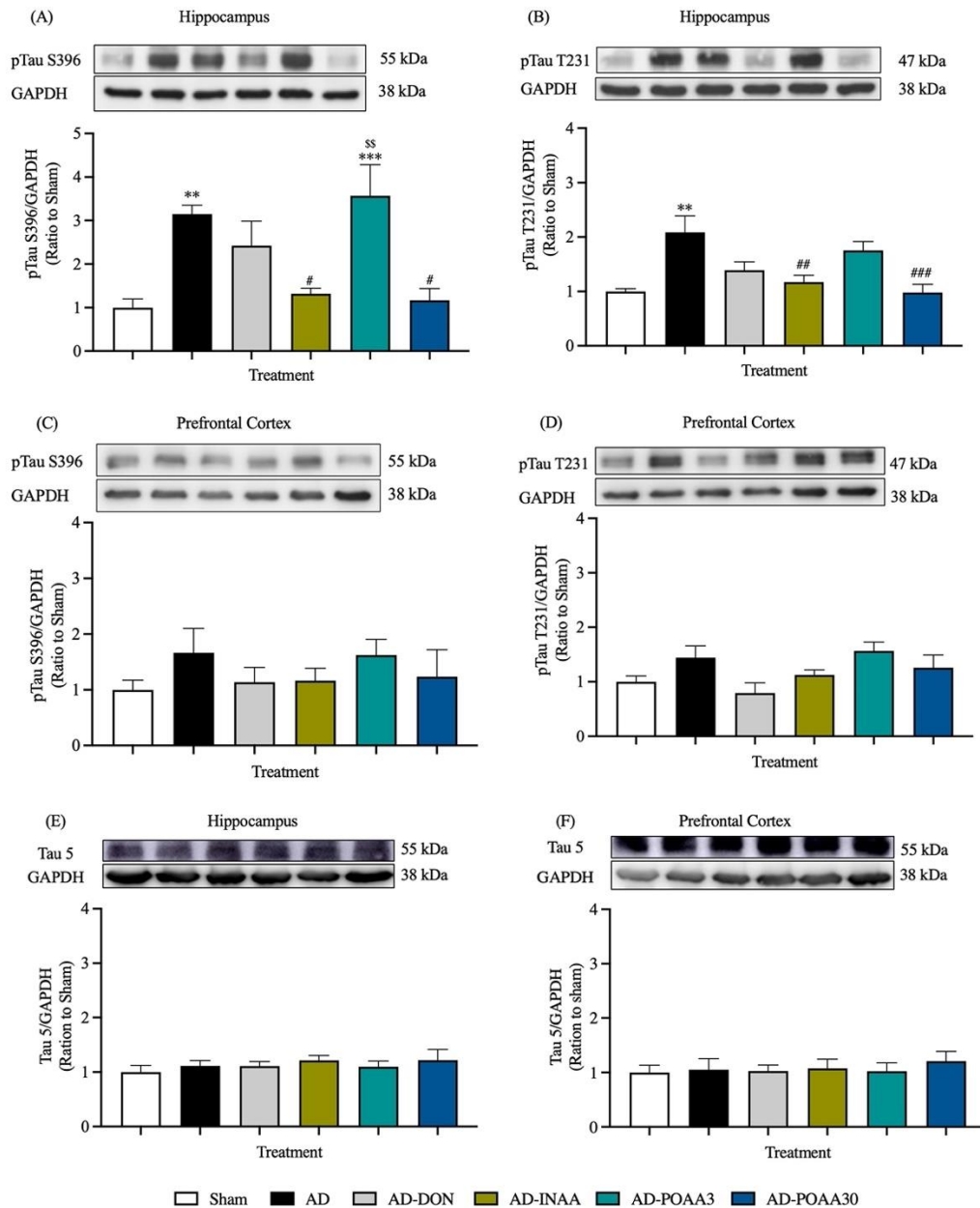


Figure 13 The effect of AA by intranasal and oral administration on tau hyperphosphorylation induced by $A\beta_{1-42}$.

(A) pTau S396 and (B) pTau T231 in the hippocampus, (C) pTau S396 and (D) pTau T231 in the prefrontal cortex, Tau 5 as total tau in (E) the hippocampus and (F) the prefrontal cortex. Data are expressed as mean + S.E.M. (n = 5-6/group). ** $p < 0.01$, *** $p < 0.001$ compared to sham; # $p < 0.05$, ## $p < 0.01$, ### $p < 0.001$ compared AD; §§ $p < 0.01$ compared to AD-INAA.

4.6 The protective effect of nasal delivery and oral administration of AA against glial activation induced by $A\beta_{1-42}$

Immunofluorescence staining was used to investigate the involvement of neuroinflammation as the potential mechanisms of asiatic acid against $A\beta_{1-42}$ induce memory dysfunction. GFAP and TMEM119 antibodies were selected as the biomarker of neuroinflammation which represents astrocytes and microglial cells, respectively. The immunoreactivity of each biomarker was detected in CA1 and CA3 subregion of mice hippocampus. In this study, hypertrophic form of astrocytes was found in the CA1 and CA3 subregion of AD mice (Figure 14A, 15A). One-way ANOVA revealed the effect of treatments on astrocytes reactivity and microglial activation in the CA1 and CA3 subregion (GFAP: $F(5, 30) = 16.78$, $p < 0.0001$ and $F(5, 26) = 4.727$, $p = 0.0033$, respectively; TMEM119: $F(5, 30) = 3.729$, $p = 0.0096$ and $F(5, 26) = 4.155$, $p = 0.0066$, respectively). The percentage area of GFAP and TMEM119 in CA1 subregion of mice in AD group were significantly higher than that in the Sham group ($p < 0.001$ and $p < 0.05$, respectively, Tukey's post-hoc test) (Figure 14B, 14C). A significant increase of GFAP-immunoreactivity was detected in CA3 subregion of mice in AD group compared to the Sham group ($p < 0.01$, Tukey's post-hoc test) (Figure 15B) while the immunoreactivity of TMEM119 in mice of the AD group tended to increase but was not significantly different from mice in the Sham group ($p = 0.0642$, Tukey's post-hoc test) (Figure 15C). The treatment of AA in SLNs by nasal delivery was significantly

reduced the percentage area of GFAP and TMEM119 in the CA1 and CA3 subregion compared to mice in the AD group (GFAP: $p < 0.001$ and $p < 0.01$, respectively; TMEM119: $p < 0.05$ and $p < 0.05$, respectively, Tukey's post-hoc test). GFAP immunoreactivity in CA1 and CA3 subregion of AD-POAA30 group was significantly decreased compared to the AD group ($p < 0.001$ and $p < 0.01$, respectively, Tukey's post-hoc test). TMEM119 immunoreactivity in CA1 and CA3 of AD-POAA30 tended to decrease but they were not significantly different from AD mice. In contrast, GFAP immunoreactivity in the CA1 subregion of AD-DON and AD-POAA3 group were higher significantly than that in the Sham group ($p < 0.01$ and $p < 0.01$, respectively, Tukey's post-hoc test). The percentage of GFAP in CA1 subregion of AD-POAA3 group was also significantly higher than that of AD-INAA group ($p < 0.05$, Tukey's post-hoc test). There was no significant difference on TMEM119 immunoreactivity between AD, AD-DON and AD-POAA3 group in CA1 and CA3. These findings suggested that nasal delivery and high oral dose of AA treatment inhibited neuroinflammation by preventing glial activation in the hippocampus of AD mice model.

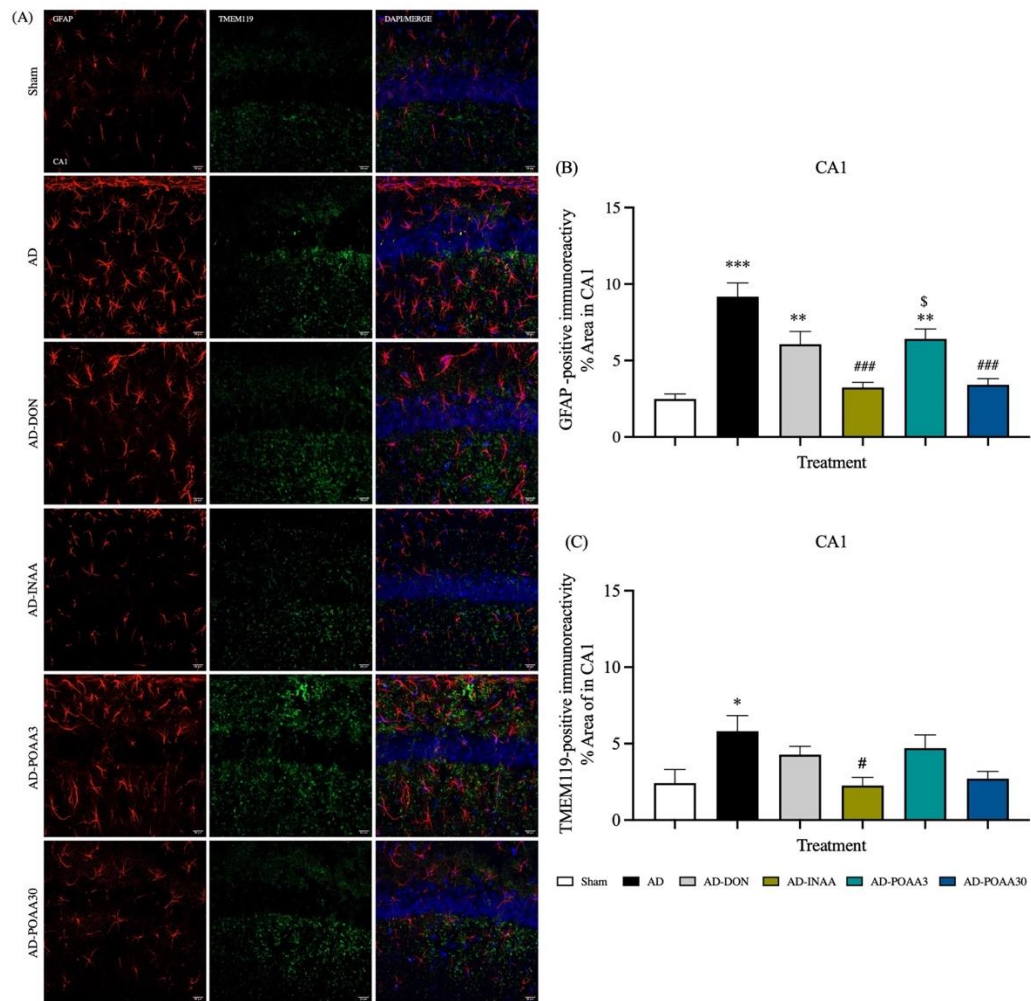


Figure 14 The effect of AA by intranasal and oral administration on glial activation induced by $A\beta_{1-42}$ in the CA1 of hippocampus.

(A) Representative micrograph showing the activation of astrocytes and microglial cells immunostaining by GFAP (red) and TMEM119 (green). Nuclei were stained with DAPI (blue). The scale bar was 20 μ m. Quantification the percentage area of GFAP (B) and TMEM119 (C) in CA1. Data are expressed as mean + S.E.M. (n = 6/group). * p < 0.05, ** p < 0.01, *** p < 0.001 compared to sham; # p < 0.05, ### p < 0.001 compared to AD; § p < 0.05 compared to AD-INAA group.

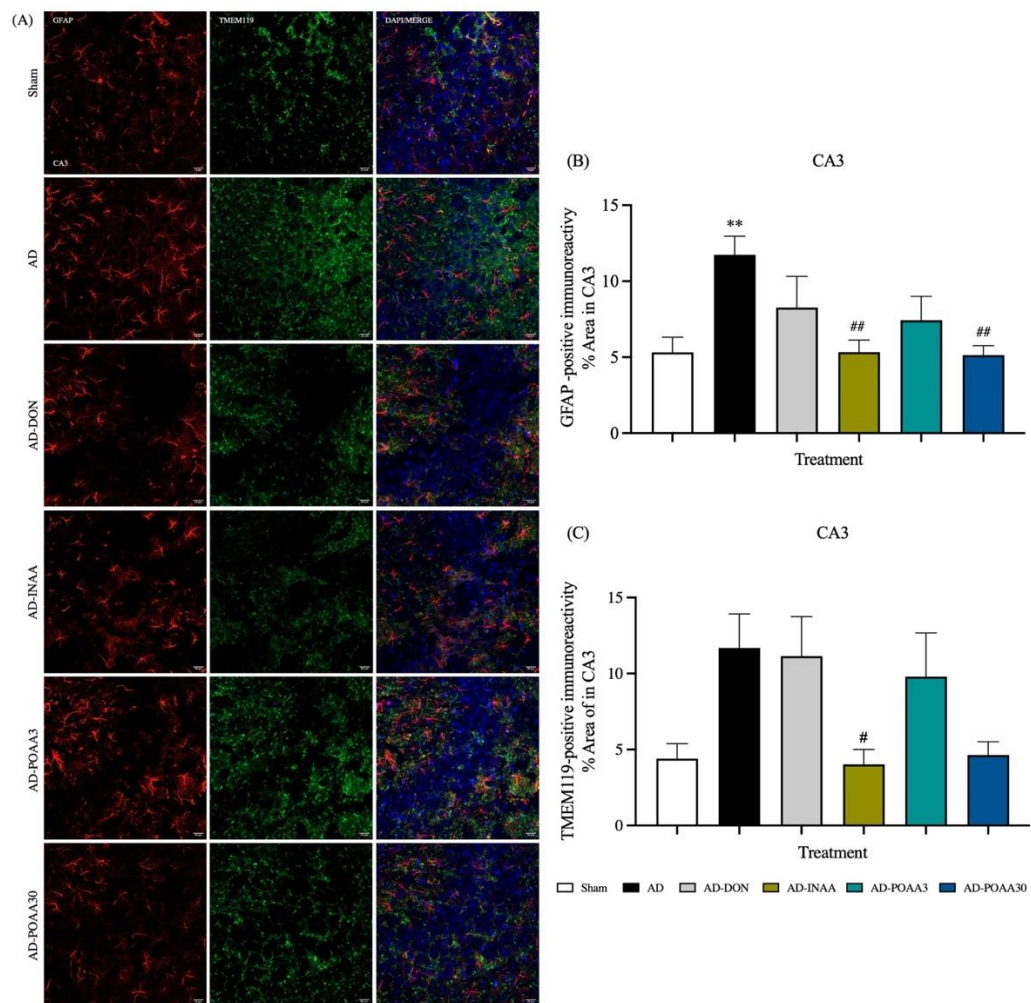


Figure 15 The effect of AA by intranasal and oral administration on glial activation induced by $A\beta_{1-42}$ in the CA3 of hippocampus.

(A) Representative micrograph showing the activation of astrocytes and microglial cells immunostaining by GFAP (red) and TMEM119 (green). Nuclei were stained with DAPI (blue). The scale bar was 20 μ m. Quantification the percentage area of GFAP (B) and TMEM119 (C) in CA3. Data are expressed as mean + S.E.M. (n = 4-6/group). ** p < 0.01 compared to sham; # p < 0.05, ## p < 0.01 compared to AD.

4.7 The protective effect of nasal delivery and oral administration of AA against the increased proinflammatory cytokines level induced by $A\beta_{1-42}$

The level of proinflammatory cytokines were measured by ELISA technique. One-way ANOVA reported the effect of treatment on IL-1 β and TNF- α levels in the brain tissue ($F(5, 29) = 23.57, p < 0.0001$ and $F(5, 29) = 15.17, p < 0.0001$, respectively). The level of IL-1 β and TNF- α of AD mice was significantly higher than that of the Sham group ($p < 0.001$ and $p < 0.0001$, respectively, Tukey's post-hoc test). Nasal delivery of AA significantly decreased IL-1 β ($p < 0.001$, Tukey's post-hoc test) but not TNF- α levels compared to the AD group while POAA30 treatment significantly reduced both of IL-1 β and TNF- α levels in AD mice brain ($p < 0.001$ and $p < 0.05$ respectively, Tukey's post-hoc test). In contrast, IL-1 β and TNF- α levels of AD mice treated with donepezil and low oral dose of AA were increased significantly compared to the Sham group (AD-DON: $p < 0.001$ and $p < 0.001$, respectively; AD-POAA3: $p < 0.001$ and $p < 0.001$, respectively, Tukey's post-hoc test). AD-POAA3 mice also had significantly higher IL-1 β and TNF- α levels than AD-INAA mice ($p < 0.001$ and $p < 0.05$, respectively, Tukey's post-hoc test) (Figure 16A, 16B). Taken together, these results indicated that nasal delivery and high oral dose of AA inhibited the release of proinflammatory cytokines in AD mice model.

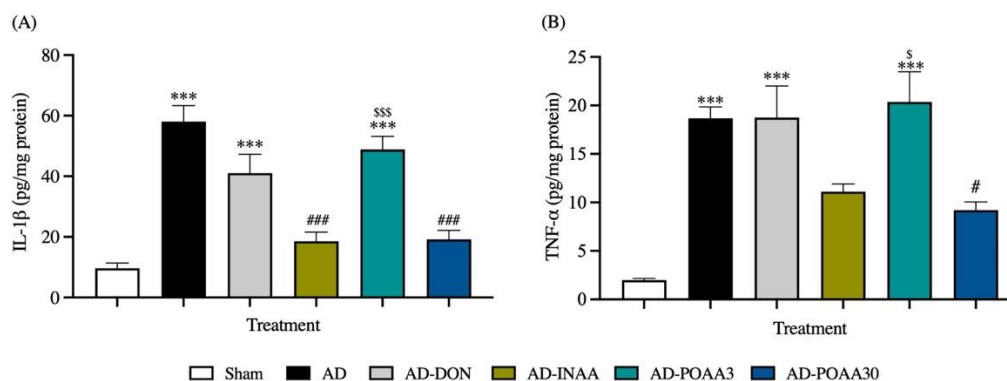


Figure 16 The effect of AA by intranasal and oral administration on the increased IL-1 β (A) and TNF- α (B) levels induced by A β ₁₋₄₂.

Data are expressed as mean + S.E.M. (n = 5-6/group). *** p < 0.001 compared to sham; # p < 0.05, ### p < 0.001 compared to AD; \$ p < 0.05, \$\$\$ p < 0.001 compared to AD-INAA.

4.8 The protective effect of nasal delivery and oral administration of AA against lipid peroxidation induced by A β ₁₋₄₂

Malondialdehyde (MDA), a lipid peroxidation marker, was detected in the brain tissue by TBARS method. One-way ANOVA revealed the effect of treatment on MDA levels (F (5, 27) = 6.746, p = 0.0003, Tukey's post hoc test). MDA levels of mice in AD, AD-DON and AD-POAA3 groups were significantly higher than that of the Sham group (p < 0.01, p < 0.05 and p < 0.05, respectively, Tukey's post-hoc test). MDA levels of AD-INAA and AD-POAA30 group were decreased significantly compared to AD group (p < 0.05 and p < 0.05, respectively, Tukey's post-hoc test) (Figure 17).

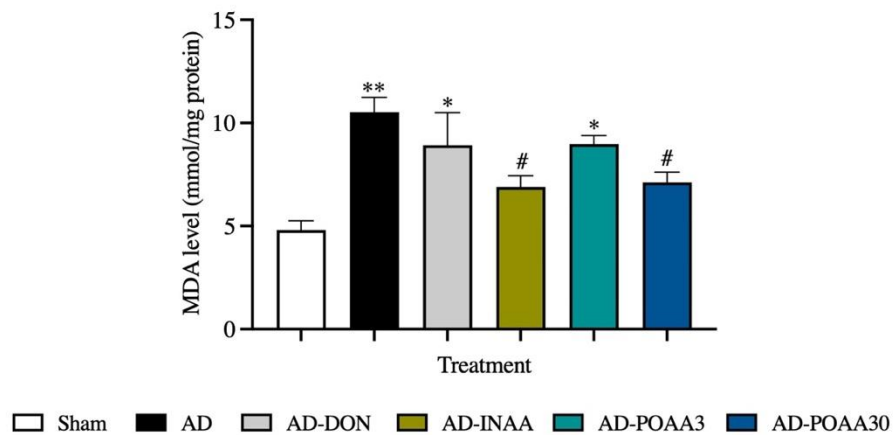


Figure 17 The effect of AA by intranasal and oral administration on MDA levels in the mice brain induced by $A\beta_{1-42}$.

Data are expressed as mean + S.E.M. (n = 5-6/group). * $p < 0.05$, ** $p < 0.01$ compared to sham; # $p < 0.05$ compared to AD (one-way ANOVA followed by Tukey's post-hoc test).

4.9 The effect of $A\beta_{1-42}$ and AA treatment on the neuronal cell counts

Nissl staining was used to determine the number of surviving neurons in mice hippocampus. There was no significant difference on the neuronal number in the CA1 and CA3 of hippocampus among experimental groups, suggesting that the injection of $A\beta_{1-42}$ oligomers did not induce neuronal loss in the hippocampus (Figure 18A, 18B, 18C).

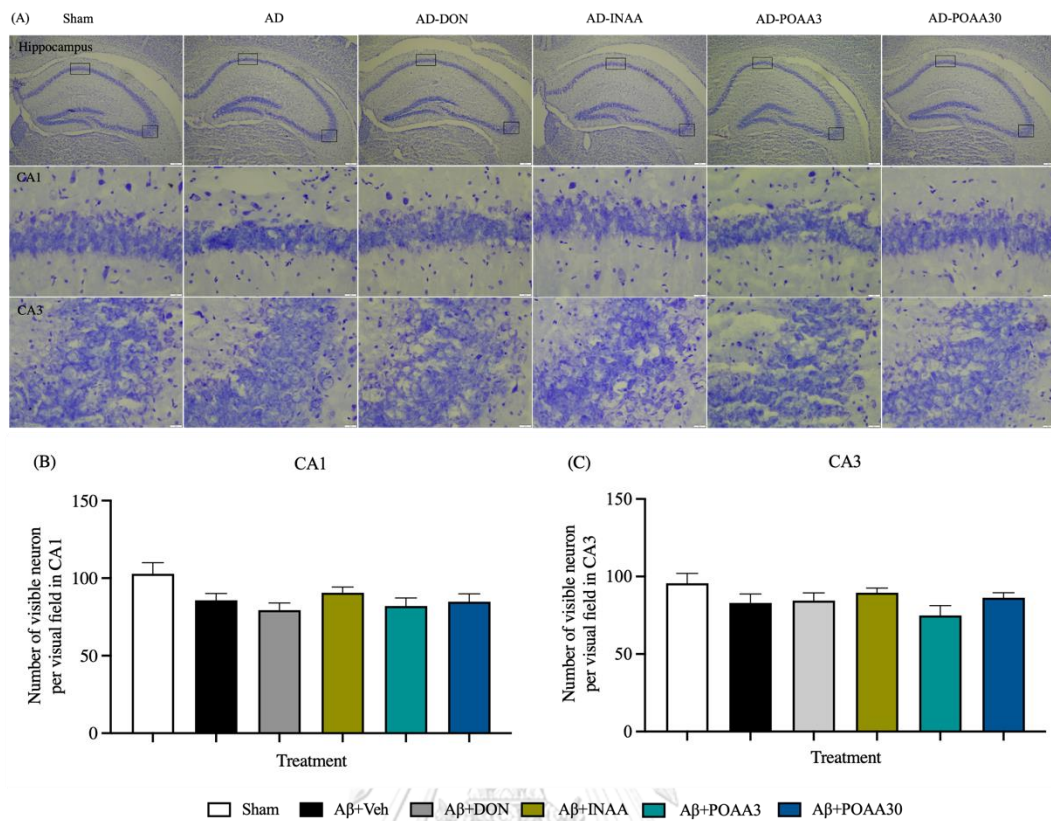


Figure 18 The effect $A\beta_{1-42}$ injection and AA treatment on the neuronal counts in the hippocampus.

(A) Representative image of Nissl staining in the hippocampus. The scale bar was 200 μm in the overview image and 20 μm in the detail image of hippocampus subregions (CA1 and CA3). The number of visible neurons in the CA1 (B) and CA3 (C) subregion. Data are expressed as mean + S.E.M. (n = 6/group).

CHAPTER 5

DISCUSSION AND CONCLUSION

The current study aimed to investigate the neuroprotective effects and the underlying mechanisms of nasal delivery of asiatic acid (AA) against $A\beta_{1-42}$ induced neurotoxicity in mice as an *in vivo* model of Alzheimer's disease. It was showed that the treatment of AA by nasal delivery ameliorated spatial memory and recognition memory deficits in mice. The neuroprotective effect of AA by nasal delivery (dose) was similar to the oral dose of AA (30 mg/kg), while lower oral dose of AA (3 mg/kg) failed to protect the neurotoxic effect of $A\beta_{1-42}$. The neuroprotective effects of AA mediated through the inhibition of hyperphosphorylated tau, glial activation, proinflammatory cytokines release, lipid peroxidation in mice brains.

The immunohistological staining showed the distribution of $A\beta_{1-42}$ deposits in mice hippocampus after intraventricular injection. The aggregated $A\beta_{1-42}$ were confirmed under light microscope observation before injected to the animals as previously described¹²². Previous study demonstrated that four days incubation at 37°C of $A\beta_{25-35}$ peptides in sterile distilled water formed two types of aggregated forms: globular aggregates and birefringent fibril-like structures¹²². In the present study, the compositions of oligomer and monomer form of $A\beta_{1-42}$ were found predominantly after 96 h incubation of soluble $A\beta_{1-42}$ fragments. A previous study showed that the monomer and oligomer form of $A\beta_{1-42}$ without fibril formation were

observed after 16 h incubation at 4°C¹²³. However, fibril formation was found in our preparations. Several factors can affect the aggregation process of A β ₁₋₄₂ including pre-existing structure of commercial stock, amyloid beta species, the incubation condition such as time, temperature, pH, concentration, solvent, and ionic strength¹²³. In this study, a qualitative analysis with immunohistochemistry technique was done to show the distribution of A β ₁₋₄₂ in mice hippocampus. Human A β ₁₋₄₂ fragments were injected into mice brain, but an unspecific species of A β ₁₋₄₂ polyclonal antibody was used to stain the brain tissue. Because the antibody can detect the A β ₁₋₄₂ of mice, the limitation this study that human and mouse A β ₁₋₄₂ cannot be distinguished.

Nose-to-brain delivery of AA (2.04 ± 0.16 mg/kg) exhibited memory improvement in A β ₁₋₄₂ induced mice model of Alzheimer's disease. High oral dose of AA (30 mg/kg) also showed a significant improvement in memory functions, indicating that AA protected against A β ₁₋₄₂-induced memory impairment. These findings are in consistent with previous studies reporting that AA improved memory performance in AlCl₃⁶, quinolinic acid¹¹, 5-fluorouracil¹², valproate¹³, and scopolamine³² induced memory dysfunction in animals. AA showed a nootropic effect after oral administration for 28 days in rats¹²⁴. In addition, *Centella asiatica* extract (600 mg/kg) for 14 days increased the expression levels of NMDA receptor subunit GluN2B (NR2B), but decreased the expression levels of NMDA receptor subunit GluN2A (NR2A) in the

rat brain¹²⁵. The activation of NR2B-containing NMDA receptor is higher than NR2A-containing receptor during the long-term potentiation (LTP)³⁵. Therefore, AA-induced LTP might be served as one of the mechanisms that improves learning and memory impairment due to the exposure of A β ₁₋₄₂.

Intranasal administration of AA in SLNs (2.04 \pm 0.16 mg/kg) has a greater neuroprotective effect than oral administration of AA (3 mg/kg). AA and SLNs had a lipophilic property which is beneficial for drug-brain delivery. Due to lipophilic nature of SLNs, it has been suggested that SLNs can pass through the nasal epithelium by passive diffusion mechanism¹²⁶. After reaching nasal epithelium, SLNs might be transported directly to the brain using the axonal transport along the olfactory and trigeminal nerves as intraneuronal pathway¹⁰⁴. Drug molecules might be uptaken into the olfactory and trigeminal sensory neurons by several mechanisms including transcellular, transcytosis and carrier-mediated transport depend on their sizes and molecular characteristics¹⁰⁴. Recently, *in vitro* study showed the axonal retrograde transport of nanoparticles in the neurons¹²⁷. It has been proven that negative charge of nanoparticles were used rapid growth cone uptake and dynein-axonal retrograde transport depends on the size and cell type¹²⁷. Then, as a controlled released design, the release of AA from the matrix of SLNs might be through several mechanism such as direct drug diffusion through the matrix, rapid release due to weak bound with SLN surface, and erosion of SLN matrix due to enzymatic reaction

by lipase or colipase^{118,128}. Those release mechanisms were affected by the formulation and biological environment.

Therefore, we hypothesized that AA in SLNs use passive diffusion mechanism to cross nasal epithelium in the nasal cavity¹²⁹. The axonal transport along the olfactory and respiratory nerves is the main intracellular mechanisms to deliver drug molecule into the brain tissue. The average size of axonal diameter in mice brain can be vary between less than 0.2 μm and 10.0 μm ¹⁰⁷, while 3-months old ICR mice had the olfactory axonal diameter range from 0.08 to 0.14 μm in the lamina propria¹¹¹. Therefore, only molecules within or smaller than these sizes can be transported along this mechanism. Since the average particles size of SLNs is around 100-300 nm¹¹³, we hypothesized that AA in SLNs uses the neuronal pathway to achieve its efficacy in AD mice.

AA inhibited tau hyperphosphorylation induced by $A\beta_{1-42}$ in mice hippocampus. In this study, $A\beta_{1-42}$ significantly promoted tau hyperphosphorylation in the hippocampus rather than in the prefrontal cortex, while AA administration by either nasal delivery or high oral dose significantly reduced hyperphosphorylated tau protein induced by $A\beta_{1-42}$ mainly in the hippocampus tissue. The previous study in rats showed that AA inhibited AlCl_3 -induced hyperphosphorylated tau protein by interfering AKT/GSK3 β pathway¹⁰⁰. The study in PC12 cells also revealed that AA reduced tau hyperphosphorylation induced by $A\beta_{25-35}$ via the AKT/GSK3 β

pathway¹³⁰. Further study are need to elucidate whether the modulation of AKT/GSK3 β pathway is one of the mechanisms of the prevention effect of AA on hyperphosphorylated tau protein induced by A β ₁₋₄₂.

AA prevented neuroinflammation induced by A β ₁₋₄₂ in mice hippocampus. Neuroinflammation involves astrocytes and microglial accumulations followed by the release of proinflammatory cytokines in the AD brain of animals and humans^{131,132}. This study demonstrated that A β ₁₋₄₂ stimulated astrocyte and microglial reactivation especially in CA1 subregion of the hippocampus. Meanwhile, INAA significantly prevented both glial activation in CA1 and CA3 subregions followed by the reduction of IL-1 β and TNF- α levels in mice brain. Anti-neuroinflammatory effect of AA involved several mechanisms. AA bound to the active site of IL-1 β and IL-6 receptors by *in silico* study¹³³. AA reduced IL-1 β , IL-6 and TNF- α levels induced by lipopolysaccharide (LPS) in BV2 microglial cells¹³⁴. Another *in vivo* study reported that AA not only reduced IL-1 β and TNF- α levels but also decreased TLR2 and TLR4 receptor expression in the striatum of MPTP-treated mice¹³⁵. Therefore, the modulation of TLR receptors or direct interaction with proinflammatory cytokine receptors might be mediated anti-neuroinflammatory effect of AA. Chronic neuronal inflammation in the brain could promote tau hyperphosphorylation and LTP inhibition leading to synaptic dysfunction^{59,77,78}. High expression of phosphorylated tau protein in this study might be affected by the neuroinflammatory reactions in the

mice brain. Therefore, anti-neuroinflammatory effect of AA possibly contributes to the reduction of hyperphosphorylation tau protein in AD mice.

Repeated administration of AA by nasal delivery system decreased lipid peroxidation. Oxidative stress plays an important role in the progress of Alzheimer's disease⁸³. The previous studies revealed the antioxidant effect of AA in cognitive dysfunction rat model induced by quinolinic acid¹¹ and aluminium chloride (AlCl₃)¹⁰. In those studies, AA increased the expression of antioxidant enzymes such as superoxide dismutase (SOD), catalase (CAT), and glutathione peroxidase (GPx) accompanied by the reduction of MDA level in rat brains^{10,11}. Intranasal administration of AA in SLNs increased catalase expression in mice hippocampus and decreased MDA level in mice brain in the scopolamine model³². Tau hyperphosphorylation can be also stimulated by oxidative stress⁸⁷. Therefore, the reduction of tau hyperphosphorylation by AA treatment in this study is possibly associated with the anti-oxidant effect of AA.

Our study revealed no anxiety-like behaviour induced by A β ₁₋₄₂ in the open-field and elevated plus maze tasks. The previous study also showed that A β ₁₋₄₂ -induced AD mice did not exhibit anxiety-like behaviour after two-week A β ₁₋₄₂ injection in elevated plus maze¹³⁶. In contrast, the time spent in the open arms was increased significantly after three-week of A β ₁₋₄₂ injection¹³⁶. Anxiety-like behaviour was also not seen in the transgenic mice model (APP/PS1 knock-in) at any age in

open-field and elevated plus maze tests¹³⁷. Our results are in contrast with previous studies as AD mice increased anxiety-related behaviour, suggesting inconsistent profile of anxiety-like behaviour in the animal models of AD. Several factors including measurement time point, the aged and model of animal might be affected the anxiety-like behaviour analysis. In addition, the underlying mechanism of A β ₁₋₄₂ - induced anxiety-like behaviour remains unclear.

Amyloid beta₁₋₄₂ oligomers did not induce hippocampal neuronal loss in this study. This is in consistent with the previous study showing that bilateral intrahippocampal injection of A β ₁₋₄₂ oligomers successfully induced memory impairment and neuroinflammation in AD rat brain but did not stimulate cause neuronal death in the hippocampus¹²³. Another study also found that A β ₁₋₄₂ oligomers induced spatial memory dysfunction and reduced LTP in rat brain but did not reduce neuron number in the hippocampus¹³⁸. In addition, there was no significant difference between rat-treated A β ₁₋₄₂ versus control group on the NeuN-positive cells number in the hippocampus, while AD rat model significantly reduced LTP in dentate gyrus and impaired the spatial memory¹³⁹. In the previous study, neuronal loss was not found in the hippocampus in several AD transgenic mice (JNPL3, 5xFAD, and 6xTg mice) at 2 and 4 months old while the number of amyloid beta plaque and neuroinflammation marker were increased significantly on that age as compared with the wild type mice¹⁴⁰. The significant neuronal loss in the

hippocampus of all AD transgenic mice was found at 6 and 8 months old¹⁴⁰. Therefore, no significant loss in the hippocampus in this study might be affected by the age of the animal. It was hypothesized that amyloid beta induced memory dysfunction due to the malfunctions of synaptic plasticity that interfered signal transduction in memory-specific region rather than neuronal cell loss¹⁴¹. Therefore, our model is also likely suitable to induce the early stage of AD in rodent.

In conclusion, intranasal administration of AA in SLNs exhibited a neuroprotective effect in the amyloid beta₁₋₄₂ model of Alzheimer's disease. The neuroprotective mechanisms of AA involved in the prevention of tau hyperphosphorylation, the inhibition of neuroinflammation, and the reduction of oxidative stress. Therefore, the involvement of synaptogenesis in the neuroprotective mechanism of AA should be investigated for future study.

REFERENCES



จุฬาลงกรณ์มหาวิทยาลัย
CHULALONGKORN UNIVERSITY

- 1 Yin, X. *et al.* The Role of Amyloid-Beta and Tau in the Early Pathogenesis of Alzheimer's Disease. *Med Sci Monit* **27**, e933084 (2021).
<https://doi.org/10.12659/msm.933084>
- 2 Niikura, T., Tajima, H. & Kita, Y. Neuronal cell death in Alzheimer's disease and a neuroprotective factor, humanin. *Curr Neuropharmacol* **4**, 139-147 (2006).
<https://doi.org/10.2174/157015906776359577>
- 3 Song, T. *et al.* Mitochondrial dysfunction, oxidative stress, neuroinflammation, and metabolic alterations in the progression of Alzheimer's disease: A meta-analysis of in vivo magnetic resonance spectroscopy studies. *Ageing Research Reviews* **72**, 101503 (2021). <https://doi.org/10.1016/j.arr.2021.101503>
- 4 Tönnies, E. & Trushina, E. Oxidative Stress, Synaptic Dysfunction, and Alzheimer's Disease. *J Alzheimers Dis* **57**, 1105-1121 (2017).
<https://doi.org/10.3233/jad-161088>
- 5 Yiannopoulou, K. G. & Papageorgiou, S. G. Current and Future Treatments in Alzheimer Disease: An Update. *Journal of central nervous system disease* **12**, 1179573520907397-1179573520907397 (2020).
<https://doi.org/10.1177/1179573520907397>

- 6 Ahmad Rather, M. *et al.* Asiatic acid nullified aluminium toxicity in in vitro model of Alzheimer's disease. *Front Biosci (Elite Ed)* **10**, 287-299 (2018). <https://doi.org/10.2741/e823>
- 7 Lee, M. K. *et al.* Asiatic acid derivatives protect cultured cortical neurons from glutamate-induced excitotoxicity. *Res Commun Mol Pathol Pharmacol* **108**, 75-86 (2000).
- 8 Xu, M. F. *et al.* Asiatic acid, a pentacyclic triterpene in *Centella asiatica*, attenuates glutamate-induced cognitive deficits in mice and apoptosis in SH-SY5Y cells. *Acta Pharmacol Sin* **33**, 578-587 (2012). <https://doi.org/10.1038/aps.2012.3>
- 9 Park, J.-H. *et al.* Asiatic acid attenuates methamphetamine-induced neuroinflammation and neurotoxicity through blocking of NF- κ B/STAT3/ERK and mitochondria-mediated apoptosis pathway. *Journal of Neuroinflammation* **14**, 240 (2017). <https://doi.org/10.1186/s12974-017-1009-0>
- 10 Suryavanshi, J., Prakash, C. & Sharma, D. Asiatic acid attenuates aluminium chloride-induced behavioral changes, neuronal loss and astrocyte activation in rats. *Metab Brain Dis* **37**, 1773-1785 (2022). <https://doi.org/10.1007/s11011-022-00998-3>
- 11 Loganathan, C. & Thayumanavan, P. Asiatic acid prevents the quinolinic acid-induced oxidative stress and cognitive impairment. *Metab Brain Dis* **33**, 151-159 (2018). <https://doi.org/10.1007/s11011-017-0143-9>

- 12 Chaisawang, P. *et al.* Asiatic acid protects against cognitive deficits and reductions in cell proliferation and survival in the rat hippocampus caused by 5-fluorouracil chemotherapy. *PLOS ONE* **12**, e0180650 (2017). <https://doi.org/10.1371/journal.pone.0180650>
- 13 Umka Welbat, J. *et al.* Asiatic Acid Prevents the Deleterious Effects of Valproic Acid on Cognition and Hippocampal Cell Proliferation and Survival. *Nutrients* **8** (2016). <https://doi.org/10.3390/nu8050303>
- 14 Yuan, Y. *et al.* Biopharmaceutical and pharmacokinetic characterization of asiatic acid in *Centella asiatica* as determined by a sensitive and robust HPLC-MS method. *J Ethnopharmacol* **163**, 31-38 (2015). <https://doi.org/10.1016/j.jep.2015.01.006>
- 15 Lochhead, J. J. & Thorne, R. G. Intranasal delivery of biologics to the central nervous system. *Adv Drug Deliv Rev* **64**, 614-628 (2012). <https://doi.org/10.1016/j.addr.2011.11.002>
- 16 Baltzley, S., Mohammad, A., Malkawi, A. H. & Al-Ghananeem, A. M. Intranasal drug delivery of olanzapine-loaded chitosan nanoparticles. *AAPS PharmSciTech* **15**, 1598-1602 (2014). <https://doi.org/10.1208/s12249-014-0189-5>
- 17 Shah, B., Khunt, D., Bhatt, H. S., Misra, M. & Padh, H. Intranasal delivery of venlafaxine loaded nanostructured lipid carrier: Risk assessment and QbD

- based optimization. *Journal of Drug Delivery Science and Technology* **33**, 37-50 (2016).
- 18 Liu, S., Yang, S. & Ho, P. C. Intranasal administration of carbamazepine-loaded carboxymethyl chitosan nanoparticles for drug delivery to the brain. *Asian J Pharm Sci* **13**, 72-81 (2018). <https://doi.org:10.1016/j.ajps.2017.09.001>
- 19 Espinoza, L. C. *et al.* Formulation Strategies to Improve Nose-to-Brain Delivery of Donepezil. *Pharmaceutics* **11** (2019). <https://doi.org:10.3390/pharmaceutics11020064>
- 20 Hogan, R. E. *et al.* Bioavailability and safety of diazepam intranasal solution compared to oral and rectal diazepam in healthy volunteers. *Epilepsia* **61**, 455-464 (2020). <https://doi.org:10.1111/epi.16449>
- 21 Zelcer, M. & Goldman, R. D. Intranasal midazolam for seizure cessation in the community setting. *Can Fam Physician* **62**, 559-561 (2016).
- 22 Novak, P., Pimentel Maldonado, D. A. & Novak, V. Safety and preliminary efficacy of intranasal insulin for cognitive impairment in Parkinson disease and multiple system atrophy: A double-blinded placebo-controlled pilot study. *PLoS One* **14**, e0214364 (2019). <https://doi.org:10.1371/journal.pone.0214364>
- 23 Derad, I. *et al.* Intranasal angiotensin II in humans reduces blood pressure when angiotensin II type 1 receptors are blocked. *Hypertension* **63**, 762-767 (2014). <https://doi.org:10.1161/hypertensionaha.113.02860>

- 24 Hallschmid, M., Smolnik, R., McGregor, G., Born, J. & Fehm, H. L. Overweight humans are resistant to the weight-reducing effects of melanocortin4-10. *J Clin Endocrinol Metab* **91**, 522-525 (2006). <https://doi.org/10.1210/jc.2005-0906>
- 25 Guastella, A. J. *et al.* Intranasal oxytocin improves emotion recognition for youth with autism spectrum disorders. *Biol Psychiatry* **67**, 692-694 (2010). <https://doi.org/10.1016/j.biopsych.2009.09.020>
- 26 Baier, P. C. *et al.* Olfactory dysfunction in patients with narcolepsy with cataplexy is restored by intranasal Orexin A (Hypocretin-1). *Brain* **131**, 2734-2741 (2008). <https://doi.org/10.1093/brain/awn193>
- 27 Tapeinos, C., Battaglini, M. & Ciofani, G. Advances in the design of solid lipid nanoparticles and nanostructured lipid carriers for targeting brain diseases. *J Control Release* **264**, 306-332 (2017). <https://doi.org/10.1016/j.jconrel.2017.08.033>
- 28 Yasir, M. *et al.* Solid lipid nanoparticles for nose to brain delivery of donepezil: formulation, optimization by Box–Behnken design, in vitro and in vivo evaluation. *Artificial Cells, Nanomedicine, and Biotechnology* **46**, 1838-1851 (2018). <https://doi.org/10.1080/21691401.2017.1394872>
- 29 Yasir, M. & Sara, U. V. Solid lipid nanoparticles for nose to brain delivery of haloperidol: in vitro drug release and pharmacokinetics evaluation. *Acta Pharm Sin B* **4**, 454-463 (2014). <https://doi.org/10.1016/j.apsb.2014.10.005>

- 30 Patel, S. *et al.* Brain targeting of risperidone-loaded solid lipid nanoparticles by intranasal route. *J Drug Target* **19**, 468-474 (2011).
<https://doi.org/10.3109/1061186x.2010.523787>
- 31 Khunathum, P. *Development of asiatic acid solid lipid nanoparticles for nasal delivery* Master thesis, Chulalongkorn University, (2011).
- 32 Myint, S. L. L. *Protective Effect of Intranasal Asiatic Acid in Scopolamine-induced Memory Impairment in Mice* Master thesis, Chulalongkorn University, (2021).
- 33 Camina, E. & Güell, F. The Neuroanatomical, Neurophysiological and Psychological Basis of Memory: Current Models and Their Origins. *Frontiers in Pharmacology* **8** (2017). <https://doi.org/10.3389/fphar.2017.00438>
- 34 Cotton, K. & Ricker, T. J. Working memory consolidation improves long-term memory recognition. *J Exp Psychol Learn Mem Cogn* **47**, 208-219 (2021).
<https://doi.org/10.1037/xlm0000954>
- 35 Bear, M. C., BW; Paradiso, MA. *Neuroscience : exploring the brain*. (Wolters Kluwer, 2016).
- 36 Jin, J. & Maren, S. Prefrontal-Hippocampal Interactions in Memory and Emotion. *Frontiers in Systems Neuroscience* **9** (2015).
<https://doi.org/10.3389/fnsys.2015.00170>

- 37 Bird, C. M. & Burgess, N. The hippocampus and memory: insights from spatial processing. *Nature Reviews Neuroscience* **9**, 182-194 (2008).
<https://doi.org/10.1038/nrn2335>
- 38 Wirt, R. A. & Hyman, J. M. Integrating Spatial Working Memory and Remote Memory: Interactions between the Medial Prefrontal Cortex and Hippocampus. *Brain Sci* **7** (2017). <https://doi.org/10.3390/brainsci7040043>
- 39 Sigurdsson, T. & Duvarci, S. Hippocampal-Prefrontal Interactions in Cognition, Behavior and Psychiatric Disease. *Front Syst Neurosci* **9**, 190 (2015).
<https://doi.org/10.3389/fnsys.2015.00190>
- 40 Ghafarimoghadam, M. *et al.* A review of behavioral methods for the evaluation of cognitive performance in animal models: Current techniques and links to human cognition. *Physiology & Behavior* **244**, 113652 (2022).
<https://doi.org/10.1016/j.physbeh.2021.113652>
- 41 Bromley-Brits, K., Deng, Y. & Song, W. Morris water maze test for learning and memory deficits in Alzheimer's disease model mice. *J Vis Exp* (2011).
<https://doi.org/10.3791/2920>
- 42 Vorhees, C. V. & Williams, M. T. Morris water maze: procedures for assessing spatial and related forms of learning and memory. *Nature Protocols* **1**, 848-858 (2006). <https://doi.org/10.1038/nprot.2006.116>
- 43 Lueptow, L. M. Novel Object Recognition Test for the Investigation of Learning and Memory in Mice. *J Vis Exp* (2017). <https://doi.org/10.3791/55718>

- 44 Sivakumaran, M. H., Mackenzie, A. K., Callan, I. R., Ainge, J. A. & O'Connor, A. R. The Discrimination Ratio derived from Novel Object Recognition tasks as a Measure of Recognition Memory Sensitivity, not Bias. *Scientific Reports* **8**, 11579 (2018). <https://doi.org/10.1038/s41598-018-30030-7>
- 45 Association, A. s. 2022 Alzheimer's Disease Facts and Figures. (2022).
- 46 Bekris, L. M., Yu, C. E., Bird, T. D. & Tsuang, D. W. Genetics of Alzheimer disease. *J Geriatr Psychiatry Neurol* **23**, 213-227 (2010). <https://doi.org/10.1177/0891988710383571>
- 47 R, A. A. Risk factors for Alzheimer's disease. *Folia Neuropathol* **57**, 87-105 (2019). <https://doi.org/10.5114/fn.2019.85929>
- 48 Gunawardena, I. P. C., Retinasamy, T. & Shaikh, M. F. Is Aducanumab for LMICs? Promises and Challenges. *Brain Sciences* **11**, 1547 (2021).
- 49 Kumar, V., Abbas, A. K., Aster, J. C., & Robbins, S. L. *Robbins basic pathology*. (PA: Elsevier/Saunders, 2013).
- 50 Mawuenyega, K. G. *et al.* Decreased clearance of CNS beta-amyloid in Alzheimer's disease. *Science* **330**, 1774 (2010). <https://doi.org/10.1126/science.1197623>
- 51 Sun, X., Chen, W. D. & Wang, Y. D. β -Amyloid: the key peptide in the pathogenesis of Alzheimer's disease. *Front Pharmacol* **6**, 221 (2015). <https://doi.org/10.3389/fphar.2015.00221>

- 52 Schmidt, M. *et al.* Comparison of Alzheimer A β (1–40) and A β (1–42) amyloid fibrils reveals similar protofilament structures. *Proceedings of the National Academy of Sciences* **106**, 19813-19818 (2009). <https://doi.org/doi:10.1073/pnas.0905007106>
- 53 Näslund, J. *et al.* Relative abundance of Alzheimer A beta amyloid peptide variants in Alzheimer disease and normal aging. *Proc Natl Acad Sci U S A* **91**, 8378-8382 (1994). <https://doi.org/10.1073/pnas.91.18.8378>
- 54 Chen, Y. G. Research Progress in the Pathogenesis of Alzheimer's Disease. *Chin Med J (Engl)* **131**, 1618-1624 (2018). <https://doi.org/10.4103/0366-6999.235112>
- 55 Barbier, P. *et al.* Role of Tau as a Microtubule-Associated Protein: Structural and Functional Aspects. *Frontiers in Aging Neuroscience* **11** (2019). <https://doi.org/10.3389/fnagi.2019.00204>
- 56 Luna-Muñoz, J. *et al.* in *Understanding Alzheimer's Disease* Ch. 5, 89-107 (2013).  จุฬาลงกรณ์มหาวิทยาลัย
CHULALONGKORN UNIVERSITY
- 57 Kontaxi, C., Piccardo, P. & Gill, A. C. Lysine-Directed Post-translational Modifications of Tau Protein in Alzheimer's Disease and Related Tauopathies. *Front Mol Biosci* **4**, 56 (2017). <https://doi.org/10.3389/fmolb.2017.00056>
- 58 Šimić, G. *et al.* Tau Protein Hyperphosphorylation and Aggregation in Alzheimer's Disease and Other Tauopathies, and Possible Neuroprotective Strategies. *Biomolecules* **6**, 6 (2016). <https://doi.org/10.3390/biom6010006>

- 59 Xia, Y., Prokop, S. & Giasson, B. I. "Don't Phos Over Tau": recent developments in clinical biomarkers and therapies targeting tau phosphorylation in Alzheimer's disease and other tauopathies. *Mol Neurodegener* **16**, 37 (2021). <https://doi.org:10.1186/s13024-021-00460-5>
- 60 Noble, W., Hanger, D. P., Miller, C. C. & Lovestone, S. The importance of tau phosphorylation for neurodegenerative diseases. *Front Neurol* **4**, 83 (2013). <https://doi.org:10.3389/fneur.2013.00083>
- 61 Morishima-Kawashima, M. *et al.* Hyperphosphorylation of Tau in PHF. *Neurobiology of Aging* **16**, 365-371 (1995). [https://doi.org:https://doi.org/10.1016/0197-4580\(95\)00027-C](https://doi.org:https://doi.org/10.1016/0197-4580(95)00027-C)
- 62 Foidl, B. M. & Humpel, C. Differential Hyperphosphorylation of Tau-S199, -T231 and -S396 in Organotypic Brain Slices of Alzheimer Mice. A Model to Study Early Tau Hyperphosphorylation Using Okadaic Acid. *Frontiers in aging neuroscience* **10**, 113 (2018).
- 63 Barthélemy, N. R., Mallipeddi, N., Moiseyev, P., Sato, C. & Bateman, R. J. Tau Phosphorylation Rates Measured by Mass Spectrometry Differ in the Intracellular Brain vs. Extracellular Cerebrospinal Fluid Compartments and Are Differentially Affected by Alzheimer's Disease. *Front Aging Neurosci* **11**, 121 (2019). <https://doi.org:10.3389/fnagi.2019.00121>
- 64 Russell, C. L. *et al.* Comprehensive Quantitative Profiling of Tau and Phosphorylated Tau Peptides in Cerebrospinal Fluid by Mass Spectrometry

- Provides New Biomarker Candidates. *J Alzheimers Dis* **55**, 303-313 (2017).
<https://doi.org:10.3233/jad-160633>
- 65 Pachima, Y. I., Zhou, L.-y., Lei, P. & Gozes, I. Microtubule-Tau Interaction as a
 Therapeutic Target for Alzheimer's Disease. *Journal of Molecular
 Neuroscience* **58**, 145-152 (2016). <https://doi.org:10.1007/s12031-016-0715-x>
- 66 Heneka, M. T. *et al.* Neuroinflammation in Alzheimer's disease. *Lancet Neurol*
14, 388-405 (2015). [https://doi.org:10.1016/s1474-4422\(15\)70016-5](https://doi.org:10.1016/s1474-4422(15)70016-5)
- 67 Zhao, J., O'Connor, T. & Vassar, R. The contribution of activated astrocytes to
 A β production: implications for Alzheimer's disease pathogenesis. *J
 Neuroinflammation* **8**, 150 (2011). <https://doi.org:10.1186/1742-2094-8-150>
- 68 Kettenmann, H., Hanisch, U. K., Noda, M. & Verkhratsky, A. Physiology of
 microglia. *Physiol Rev* **91**, 461-553 (2011).
<https://doi.org:10.1152/physrev.00011.2010>
- 69 Ji, K., Akgul, G., Wollmuth, L. P. & Tsirka, S. E. Microglia actively regulate the
 number of functional synapses. *PLoS One* **8**, e56293 (2013).
<https://doi.org:10.1371/journal.pone.0056293>
- 70 Hickman, S. E., Allison, E. K. & El Khoury, J. Microglial dysfunction and
 defective beta-amyloid clearance pathways in aging Alzheimer's disease mice.
J Neurosci **28**, 8354-8360 (2008). [https://doi.org:10.1523/jneurosci.0616-
 08.2008](https://doi.org:10.1523/jneurosci.0616-08.2008)

- 71 Verkhatsky, A. & Nedergaard, M. Physiology of Astroglia. *Physiol Rev* **98**, 239-389 (2018). <https://doi.org/10.1152/physrev.00042.2016>
- 72 Matias, I., Morgado, J. & Gomes, F. C. A. Astrocyte Heterogeneity: Impact to Brain Aging and Disease. *Frontiers in Aging Neuroscience* **11** (2019). <https://doi.org/10.3389/fnagi.2019.00059>
- 73 Medeiros, R. & LaFerla, F. M. Astrocytes: conductors of the Alzheimer disease neuroinflammatory symphony. *Exp Neurol* **239**, 133-138 (2013). <https://doi.org/10.1016/j.expneurol.2012.10.007>
- 74 Olabarria, M., Noristani, H. N., Verkhatsky, A. & Rodríguez, J. J. Concomitant astroglial atrophy and astrogliosis in a triple transgenic animal model of Alzheimer's disease. *Glia* **58**, 831-838 (2010). <https://doi.org/10.1002/glia.20967>
- 75 Pereira Diniz, L. *et al.* Astrocyte Transforming Growth Factor Beta 1 Protects Synapses against A β Oligomers in Alzheimer's Disease Model. *The Journal of Neuroscience* **37**, 6797-6809 (2017). <https://doi.org/10.1523/jneurosci.3351-16.2017>
- 76 Olsen, M. *et al.* Astroglial Responses to Amyloid-Beta Progression in a Mouse Model of Alzheimer's Disease. *Mol Imaging Biol* **20**, 605-614 (2018). <https://doi.org/10.1007/s11307-017-1153-z>
- 77 Wang, W. Y., Tan, M. S., Yu, J. T. & Tan, L. Role of pro-inflammatory cytokines released from microglia in Alzheimer's disease. *Ann Transl Med* **3**, 136 (2015). <https://doi.org/10.3978/j.issn.2305-5839.2015.03.49>

- 78 Mishra, A., Kim, H. J., Shin, A. H. & Thayer, S. A. Synapse loss induced by interleukin-1 β requires pre- and post-synaptic mechanisms. *J Neuroimmune Pharmacol* **7**, 571-578 (2012). <https://doi.org/10.1007/s11481-012-9342-7>
- 79 Wajant, H. & Siegmund, D. TNFR1 and TNFR2 in the Control of the Life and Death Balance of Macrophages. *Frontiers in Cell and Developmental Biology* **7** (2019). <https://doi.org/10.3389/fcell.2019.00091>
- 80 Chadwick, W. *et al.* Targeting TNF-alpha receptors for neurotherapeutics. *Trends Neurosci* **31**, 504-511 (2008). <https://doi.org/10.1016/j.tins.2008.07.005>
- 81 Kitazawa, M. *et al.* Blocking IL-1 signaling rescues cognition, attenuates tau pathology, and restores neuronal β -catenin pathway function in an Alzheimer's disease model. *J Immunol* **187**, 6539-6549 (2011). <https://doi.org/10.4049/jimmunol.1100620>
- 82 Huang, W. J., Zhang, X. & Chen, W. W. Role of oxidative stress in Alzheimer's disease. *Biomed Rep* **4**, 519-522 (2016). <https://doi.org/10.3892/br.2016.630>
- 83 Cheignon, C. *et al.* Oxidative stress and the amyloid beta peptide in Alzheimer's disease. *Redox Biol* **14**, 450-464 (2018). <https://doi.org/10.1016/j.redox.2017.10.014>
- 84 Alavi Naini, S. M. & Soussi-Yanicostas, N. Tau Hyperphosphorylation and Oxidative Stress, a Critical Vicious Circle in Neurodegenerative Tauopathies?

- Oxid Med Cell Longev* **2015**, 151979 (2015).
<https://doi.org/10.1155/2015/151979>
- 85 Butterfield, D. A. Amyloid beta-peptide (1-42)-induced oxidative stress and neurotoxicity: implications for neurodegeneration in Alzheimer's disease brain. A review. *Free Radic Res* **36**, 1307-1313 (2002).
<https://doi.org/10.1080/1071576021000049890>
- 86 Kontush, A. Lipid peroxidation and Alzheimer's disease: Key role of Amyloid- β . *OCL* **13**, 46-53 (2006).
- 87 Alavi Naini, S. M. & Soussi-Yanicostas, N. Tau Hyperphosphorylation and Oxidative Stress, a Critical Vicious Circle in Neurodegenerative Tauopathies? *Oxidative Medicine and Cellular Longevity* **2015**, 151979 (2015).
<https://doi.org/10.1155/2015/151979>
- 88 Lv, H. *et al.* Asiatic Acid Exhibits Anti-inflammatory and Antioxidant Activities against Lipopolysaccharide and d-Galactosamine-Induced Fulminant Hepatic Failure. *Frontiers in Immunology* **8** (2017).
<https://doi.org/10.3389/fimmu.2017.00785>
- 89 Liu, W. H., Liu, T. C. & Mong, M. C. Antibacterial effects and action modes of asiatic acid. *Biomedicine (Taipei)* **5**, 16 (2015). <https://doi.org/10.7603/s40681-015-0016-7>
- 90 Ramachandran, V., Saravanan, R. & Senthilraja, P. Antidiabetic and antihyperlipidemic activity of asiatic acid in diabetic rats, role of HMG CoA: in

- vivo and in silico approaches. *Phytomedicine* **21**, 225-232 (2014).
<https://doi.org:10.1016/j.phymed.2013.08.027>
- 91 Bunbupha, S. *et al.* Asiatic acid alleviates cardiovascular remodelling in rats with L-NAME-induced hypertension. *Clin Exp Pharmacol Physiol* **42**, 1189-1197 (2015). <https://doi.org:10.1111/1440-1681.12472>
- 92 Lou, J. S. *et al.* Centella asiatica triterpenes for diabetic neuropathy: a randomized, double-blind, placebo-controlled, pilot clinical study. *Esper Dermatol* **20**, 12-22 (2018). <https://doi.org:10.23736/s1128-9155.18.00455-7>
- 93 Nataraj, J., Manivasagam, T., Justin Thenmozhi, A. & Essa, M. M. Neuroprotective effect of asiatic acid on rotenone-induced mitochondrial dysfunction and oxidative stress-mediated apoptosis in differentiated SH-SY5Y cells. *Nutr Neurosci* **20**, 351-359 (2017).
<https://doi.org:10.1080/1028415x.2015.1135559>
- 94 Patil, S. P., Maki, S., Khedkar, S. A., Rigby, A. C. & Chan, C. Withanolide A and asiatic acid modulate multiple targets associated with amyloid-beta precursor protein processing and amyloid-beta protein clearance. *J Nat Prod* **73**, 1196-1202 (2010). <https://doi.org:10.1021/np900633j>
- 95 Lee, K. Y., Bae, O. N., Weinstock, S., Kassab, M. & Majid, A. Neuroprotective effect of asiatic acid in rat model of focal embolic stroke. *Biol Pharm Bull* **37**, 1397-1401 (2014). <https://doi.org:10.1248/bpb.b14-00055>

- 96 Lee, K. Y. *et al.* Asiatic acid attenuates infarct volume, mitochondrial dysfunction, and matrix metalloproteinase-9 induction after focal cerebral ischemia. *Stroke* **43**, 1632-1638 (2012).
<https://doi.org/10.1161/strokeaha.111.639427>
- 97 Kumar, A., Prakash, A. & Dogra, S. Centella asiatica Attenuates D-Galactose-Induced Cognitive Impairment, Oxidative and Mitochondrial Dysfunction in Mice. *Int J Alzheimers Dis* **2011**, 347569 (2011).
<https://doi.org/10.4061/2011/347569>
- 98 Jusril, N. A., Muhamad Juhari, A. N. N., Abu Bakar, S. I., Md Saad, W. M. & Adenan, M. I. Combining In Silico and In Vitro Studies to Evaluate the Acetylcholinesterase Inhibitory Profile of Different Accessions and the Biomarker Triterpenes of Centella asiatica. *Molecules* **25** (2020).
<https://doi.org/10.3390/molecules25153353>
- 99 Cao, S. Y. *et al.* Asiatic acid inhibits LPS-induced inflammatory response in endometrial epithelial cells. *Microb Pathog* **116**, 195-199 (2018).
<https://doi.org/10.1016/j.micpath.2018.01.022>
- 100 Ahmad Rather, M. *et al.* Asiatic Acid Attenuated Aluminum Chloride-Induced Tau Pathology, Oxidative Stress and Apoptosis Via AKT/GSK-3 β Signaling Pathway in Wistar Rats. *Neurotox Res* **35**, 955-968 (2019).
<https://doi.org/10.1007/s12640-019-9999-2>

- 101 Nagoor Meeran, M. F. *et al.* Pharmacological Properties, Molecular Mechanisms, and Pharmaceutical Development of Asiatic Acid: A Pentacyclic Triterpenoid of Therapeutic Promise. *Frontiers in Pharmacology* **9** (2018).
<https://doi.org/10.3389/fphar.2018.00892>
- 102 Pan, Y. *et al.* In vitro modulatory effects on three major human cytochrome P450 enzymes by multiple active constituents and extracts of *Centella asiatica*. *J Ethnopharmacol* **130**, 275-283 (2010).
<https://doi.org/10.1016/j.jep.2010.05.002>
- 103 Xia, B. *et al.* Structural analysis of metabolites of asiatic acid and its analogue madecassic acid in zebrafish using LC/IT-MSn. *Molecules* **20**, 3001-3019 (2015).
<https://doi.org/10.3390/molecules20023001>
- 104 Bourganis, V., Kammona, O., Alexopoulos, A. & Kiparissides, C. Recent advances in carrier mediated nose-to-brain delivery of pharmaceuticals. *Eur J Pharm Biopharm* **128**, 337-362 (2018).
<https://doi.org/10.1016/j.ejpb.2018.05.009>
- 105 Erdő, F., Bors, L. A., Farkas, D., Bajza, Á. & Gizurarson, S. Evaluation of intranasal delivery route of drug administration for brain targeting. *Brain Res Bull* **143**, 155-170 (2018). <https://doi.org/10.1016/j.brainresbull.2018.10.009>
- 106 Lochhead, J. J. & Thorne, R. G. Intranasal delivery of biologics to the central nervous system. *Advanced Drug Delivery Reviews* **64**, 614-628 (2012).
[https://doi.org:https://doi.org/10.1016/j.addr.2011.11.002](https://doi.org/https://doi.org/10.1016/j.addr.2011.11.002)

- 107 Gizurarson, S. Anatomical and histological factors affecting intranasal drug and vaccine delivery. *Curr Drug Deliv* **9**, 566-582 (2012).
<https://doi.org/10.2174/156720112803529828>
- 108 Harkema, J. R., Carey, S. A. & Wagner, J. G. The nose revisited: a brief review of the comparative structure, function, and toxicologic pathology of the nasal epithelium. *Toxicol Pathol* **34**, 252-269 (2006).
<https://doi.org/10.1080/01926230600713475>
- 109 Gross, E. A., Swenberg, J. A., Fields, S. & Popp, J. A. Comparative morphometry of the nasal cavity in rats and mice. *J Anat* **135**, 83-88 (1982).
- 110 Morrison, E. E. & Costanzo, R. M. Morphology of olfactory epithelium in humans and other vertebrates. *Microsc Res Tech* **23**, 49-61 (1992).
<https://doi.org/10.1002/jemt.1070230105>
- 111 Watanabe, K., Kondo, K., Yamasoba, T. & Kaga, K. Age-related change in the axonal diameter of the olfactory nerve in mouse lamina propria. *Acta Otolaryngol Suppl*, 108-112 (2007).
<https://doi.org/10.1080/03655230701597598>
- 112 Pardeshi, C. V. & Belgamwar, V. S. Direct nose to brain drug delivery via integrated nerve pathways bypassing the blood-brain barrier: an excellent platform for brain targeting. *Expert Opin Drug Deliv* **10**, 957-972 (2013).
<https://doi.org/10.1517/17425247.2013.790887>

- 113 Silva, A. C., González-Mira, E., Lobo, J. M. & Amaral, M. H. Current progresses on nanodelivery systems for the treatment of neuropsychiatric diseases: Alzheimer's and schizophrenia. *Curr Pharm Des* **19**, 7185-7195 (2013).
<https://doi.org:10.2174/138161281941131219123329>
- 114 Cunha, S., Amaral, M. H., Lobo, J. M. S. & Silva, A. C. Lipid Nanoparticles for Nasal/Intranasal Drug Delivery. *Crit Rev Ther Drug Carrier Syst* **34**, 257-282 (2017). <https://doi.org:10.1615/CritRevTherDrugCarrierSyst.2017018693>
- 115 Tekade, R. K., Maheshwari, R., Tekade, M. & Chougule, M. B. in *Nanotechnology-Based Approaches for Targeting and Delivery of Drugs and Genes* (eds Vijay Mishra, Prashant Kesharwani, Mohd Cairul Iqbal Mohd Amin, & Arun Iyer) 256-286 (Academic Press, 2017).
- 116 Scioli Montoto, S., Muraca, G. & Ruiz, M. E. Solid Lipid Nanoparticles for Drug Delivery: Pharmacological and Biopharmaceutical Aspects. *Frontiers in Molecular Biosciences* **7** (2020). <https://doi.org:10.3389/fmolb.2020.587997>
- 117 Cacciatore, I., Ciulla, M., Fornasari, E., Marinelli, L. & Di Stefano, A. Solid lipid nanoparticles as a drug delivery system for the treatment of neurodegenerative diseases. *Expert Opin Drug Deliv* **13**, 1121-1131 (2016).
<https://doi.org:10.1080/17425247.2016.1178237>
- 118 Rawal, S. U. & Patel, M. M. in *Lipid Nanocarriers for Drug Targeting* (ed Alexandru Mihai Grumezescu) 49-138 (William Andrew Publishing, 2018).

- 119 Wang, R., Zhang, Y., Li, J. & Zhang, C. Resveratrol ameliorates spatial learning memory impairment induced by A β (1-42) in rats. *Neuroscience* **344**, 39-47 (2017). <https://doi.org:10.1016/j.neuroscience.2016.08.051>
- 120 Kim, H. Y., Lee, D. K., Chung, B. R., Kim, H. V. & Kim, Y. Intracerebroventricular Injection of Amyloid- β Peptides in Normal Mice to Acutely Induce Alzheimer-like Cognitive Deficits. *J Vis Exp* (2016). <https://doi.org:10.3791/53308>
- 121 Bonferoni, M. C. *et al.* Nanoemulsions for “Nose-to-Brain” Drug Delivery. *Pharmaceutics* **11**, 84 (2019).
- 122 Maurice, T., Lockhart, B. P. & Privat, A. Amnesia induced in mice by centrally administered beta-amyloid peptides involves cholinergic dysfunction. *Brain Res* **706**, 181-193 (1996). [https://doi.org:10.1016/0006-8993\(95\)01032-7](https://doi.org:10.1016/0006-8993(95)01032-7)
- 123 Wang, L.-S. *et al.* Cajaninstilbene Acid Ameliorates Cognitive Impairment Induced by Intrahippocampal Injection of Amyloid- β 1-42 Oligomers. *Frontiers in Pharmacology* **10** (2019). <https://doi.org:10.3389/fphar.2019.01084>
- 124 Sirichoat, A. *et al.* Effects of Asiatic Acid on Spatial Working Memory and Cell Proliferation in the Adult Rat Hippocampus. *Nutrients* **7**, 8413-8423 (2015).
- 125 Wong, J. H. *et al.* Differential expression of entorhinal cortex and hippocampal subfields α -amino-3-hydroxy-5-methyl-4-isoxazolepropionic acid (AMPA) and N-methyl-D-aspartate (NMDA) receptors enhanced learning and memory of rats following administration of *Centella asiatica*. *Biomedicine &*




- Pharmacotherapy* **110**, 168-180 (2019).
<https://doi.org/10.1016/j.biopha.2018.11.044>
- 126 Bahadur, S., Pardhi, D. M., Rautio, J., Rosenholm, J. M. & Pathak, K. Intranasal Nanoemulsions for Direct Nose-to-Brain Delivery of Actives for CNS Disorders. *Pharmaceutics* **12** (2020). <https://doi.org/10.3390/pharmaceutics12121230>
- 127 Lesniak, A. *et al.* Rapid Growth Cone Uptake and Dynein-Mediated Axonal Retrograde Transport of Negatively Charged Nanoparticles in Neurons Is Dependent on Size and Cell Type. *Small* **15**, 1803758 (2019).
<https://doi.org/10.1002/smll.201803758>
- 128 Attama, A. A. & Umeyor, C. E. The use of solid lipid nanoparticles for sustained drug release. *Ther Deliv* **6**, 669-684 (2015).
<https://doi.org/10.4155/tde.15.23>
- 129 Costantino, H. R., Illum, L., Brandt, G., Johnson, P. H. & Quay, S. C. Intranasal delivery: physicochemical and therapeutic aspects. *Int J Pharm* **337**, 1-24 (2007). <https://doi.org/10.1016/j.ijpharm.2007.03.025>
- 130 Cheng, W., Chen, W., Wang, P. & Chu, J. Asiatic acid protects differentiated PC12 cells from A β (25-35)-induced apoptosis and tau hyperphosphorylation via regulating PI3K/Akt/GSK-3 β signaling. *Life Sci* **208**, 96-101 (2018).
<https://doi.org/10.1016/j.lfs.2018.07.016>

- 131 Chun, H., Marriott, I., Lee, C. J. & Cho, H. Elucidating the Interactive Roles of Glia in Alzheimer's Disease Using Established and Newly Developed Experimental Models. *Frontiers in Neurology* **9** (2018). <https://doi.org/10.3389/fneur.2018.00797>
- 132 Kwon, H. S. & Koh, S.-H. Neuroinflammation in neurodegenerative disorders: the roles of microglia and astrocytes. *Translational Neurodegeneration* **9**, 42 (2020). <https://doi.org/10.1186/s40035-020-00221-2>
- 133 Legiawati, L., Fadilah, F., Bramono, K. & Indriatmi, W. In silico study of centella asiatica active compounds as anti-inflammatory agent by decreasing IL-1 and IL-6 activity, promoting IL-4 activity. *Journal of Pharmaceutical Sciences and Research* **10**, 2142-2147 (2018).
- 134 Qian, Y. *et al.* Asiatic acid suppresses neuroinflammation in BV2 microglia via modulation of the Sirt1/NF- κ B signaling pathway. *Food Funct* **9**, 1048-1057 (2018). <https://doi.org/10.1039/c7fo01442b>
- 135 Chao, P.-c., Lee, H.-l. & Yin, M.-c. Asiatic acid attenuated apoptotic and inflammatory stress in the striatum of MPTP-treated mice. *Food & Function* **7**, 1999-2005 (2016). <https://doi.org/10.1039/C6FO00041J>
- 136 Tamano, H., Ide, K., Adlard, P. A., Bush, A. I. & Takeda, A. Involvement of hippocampal excitability in amyloid β -induced behavioral and psychological

- symptoms of dementia. *J Toxicol Sci* **41**, 449-457 (2016).
<https://doi.org:10.2131/jts.41.449>
- 137 Webster, S. J., Bachstetter, A. D. & Van Eldik, L. J. Comprehensive behavioral characterization of an APP/PS-1 double knock-in mouse model of Alzheimer's disease. *Alzheimers Res Ther* **5**, 28 (2013). <https://doi.org:10.1186/alzrt182>
- 138 Kasza, Á. *et al.* Studies for Improving a Rat Model of Alzheimer's Disease: Icv Administration of Well-Characterized β -Amyloid 1-42 Oligomers Induce Dysfunction in Spatial Memory. *Molecules* **22**, 2007 (2017).
- 139 Yang, Y. *et al.* Rhynchophylline suppresses soluble A β 1-42-induced impairment of spatial cognition function via inhibiting excessive activation of extrasynaptic NR2B-containing NMDA receptors. *Neuropharmacology* **135**, 100-112 (2018).
- 140 Kang, S., Kim, J. & Chang, K.-A. Spatial memory deficiency early in 6xTg Alzheimer's disease mouse model. *Scientific Reports* **11**, 1334 (2021).
<https://doi.org:10.1038/s41598-020-79344-5>
- 141 Klein, W. L. Abeta toxicity in Alzheimer's disease: globular oligomers (ADDLs) as new vaccine and drug targets. *Neurochem Int* **41**, 345-352 (2002).
[https://doi.org:10.1016/s0197-0186\(02\)00050-5](https://doi.org:10.1016/s0197-0186(02)00050-5)

APPENDIX 1

Animal Use Certificate

	
Chulalongkorn University Animal Care and Use Committee	
Certificate of Project Approval	<input checked="" type="checkbox"/> Original <input type="checkbox"/> Renew
Animal Use Protocol No. 21-33-002	Approval No. 21-33-002
Protocol Title Neuroprotective effects of nanoformulation of asiatic acid nasal delivery in A β -induced memory impairments in mice	
Principal Investigator Ratchanee RODSIRI, Ph.D.	
Certification of Institutional Animal Care and Use Committee (IACUC) This project has been reviewed and approved by the IACUC in accordance with university regulations and policies governing the care and use of laboratory animals. The review has followed guidelines documented in Ethical Principles and Guidelines for the Use of Animals for Scientific Purposes edited by the National Research Council of Thailand.	
Date of Approval March 5, 2021	Date of Expiration March 4, 2023
Applicant Faculty/Institution Faculty of Pharmaceutical Sciences, Chulalongkorn University, Phyathai Road., Pathumwan BKK-THAILAND. 10330	
Signature of Chairperson  Name and Title THONGCHAI SOOKSAWATE, Ph.D. Chairman	Signature of Authorized Official  Name and Title PORNCHAI ROJSITTHISAK, Ph.D. Associate Dean (Research Affairs)
<small>The official signing above certifies that the information provided on this form is correct. The institution assumes that investigators will take responsibility, and follow university regulations and policies for the care and use of animals. This approval is subjected to assurance given in the animal use protocol and may be required for future investigations and reviews.</small>	

VITA

NAME Mr. Ridho Islamie

DATE OF BIRTH 22 July 1988

PLACE OF BIRTH Samarinda

INSTITUTIONS ATTENDED Bandung Institute of Technology

HOME ADDRESS Perum Graha Tirta - Tirta Bromelia No. 50. Waru, Sidoarjo,
Jawa Timur, Indonesia

